B lymphocytes undergo TLR2-dependent apoptosis upon Shigella infection

Katharina Nothelfer, Ellen T Arena, Laurie Pinaud, Michel Neunlist, Brian Mozeleski, Ilia Belotserkovsky, Claude Parsot, Premkumar Dinadayala, Anke Burger-Kentischer, Rubhana Raqib, et al.

B lymphocytes undergo TLR2-dependent apoptosis upon *Shigella* infection

Katharina Nothelfer,[1,2] Ellen T. Arena,[1,2] Laurie Pinaud,[1,2,3] Michel Neunlist,[4] Brian Mozeleski,[5,6] Ilia Belotserkovsky,[1,2] Claude Parsot,[1,2] Premkumar Dinadayala,[7] Anke Burger-Kentischer,[8] Rubhana Raqib,[9] Philippe J. Sansonetti,[1,2,10] and Armelle Phalipon[1,2]

[1]Institut Pasteur, INSERM U786, [2]Unité de Pathogénie Microbienne Moléculaire, 75015 Paris, France
[3]Université Paris Diderot, Sorbonne Paris Cité, Cellule Pasteur UPMC, 75013 Paris, France
[4]INSERM U913, Institut des Maladies de l'Appareil Digestif du Centre Hospitalier Universitaire de Nantes, 44093 Nantes, France
[5]Institut Pasteur, [6]INSERM U1041, Unité de Régulation Immunitaire et Vaccinologie, 75015 Paris, France
[7]Discovery Department, Sanofi Pasteur, 69280 Marcy l'Etoile, France
[8]Molekulare Biotechnologie, Fraunhofer-Institut für Grenzflächen- und Bioverfahrenstechnik IGB, 70569 Stuttgart, Germany
[9]Laboratory Sciences Division, International Centre for Diarrhoeal Diseases Research, Bangladesh (ICDDR,B), Dhaka 1000, Bangladesh
[10]Chaire de Microbiologie et Maladies Infectieuses, Collège de France, 75005 Paris, France

Antibody-mediated immunity to *Shigella*, the causative agent of bacillary dysentery, requires several episodes of infection to get primed and is short-lasting, suggesting that the B cell response is functionally impaired. We show that upon ex vivo infection of human colonic tissue, invasive *S. flexneri* interacts with and occasionally invades B lymphocytes. The induction of a type three secretion apparatus (T3SA)–dependent B cell death is observed in the human CL-01 B cell line in vitro, as well as in mouse B lymphocytes in vivo. In addition to cell death occurring in *Shigella*-invaded CL-01 B lymphocytes, we provide evidence that the T3SA needle tip protein IpaD can induce cell death in noninvaded cells. IpaD binds to and induces B cell apoptosis via TLR2, a signaling receptor thus far considered to result in activation of B lymphocytes. The presence of bacterial co-signals is required to sensitize B cells to apoptosis and to up-regulate *tlr2*, thus enhancing IpaD binding. Apoptotic B lymphocytes in contact with *Shigella*-IpaD are detected in rectal biopsies of infected individuals. This study therefore adds direct B lymphocyte targeting to the diversity of mechanisms used by *Shigella* to dampen the host immune response.

CORRESPONDENCE
Armelle Phalipon:
armelle.phalipon@pasteur.fr

Abbreviations used: ILF, isolated lymphoid follicle; LP, lamina propria; MMP, mitochondrial membrane potential; PAMP, pathogen-associated molecular pattern; p.i., post infection; SEAP, secreted alkaline phosphatase; T3SA, type three secretion apparatus.

Co-evolution with their hosts has provided pathogenic microorganisms with an impressive capacity to beneficially exploit cellular functions. Increasing evidence reveals the ability of pathogens to modulate host immunity, preventing the induction of an efficient immune response that may contribute to the clearance of primary infection and/or protection from reinfection. Whereas multiple viral mechanisms divert functions of DCs and B and T lymphocytes, a direct targeting of the adaptive immune system by pathogenic bacteria has only recently become of interest (Hornef et al., 2002; Finlay and McFadden, 2006; Sansonetti and Di Santo, 2007).

Virulent *Shigella flexneri* are highly contagious Gram-negative enteroinvasive bacteria that cause bacillary dysentery. In malnourished children in the developing world, untreated infections can be fatal. The invasive phenotype of *Shigella* relies on the presence of a type three secretion apparatus (T3SA), a needle-like structure used to translocate effector proteins from the bacterial cytoplasm to the membrane and cytoplasm of the host cell. Virulence effectors that are substrates of the T3SA manipulate host cell functions and promote the establishment of the bacterial infection (Parsot, 2009). An increasing amount of evidence suggests that *Shigella* creates a strong immunosuppressive environment in the course of infection. Antibody-mediated protection arises only after several episodes of infection, is of short duration, and is poorly efficient in limiting reinfection, particularly in young children (Raqib et al., 2002; 2000). Some reports indicate that *Shigella*-induced

The Rockefeller University Press $30.00
J. Exp. Med. 2014 Vol. 211 No. 6 1215-1229
www.jem.org/cgi/doi/10.1084/jem.20130914

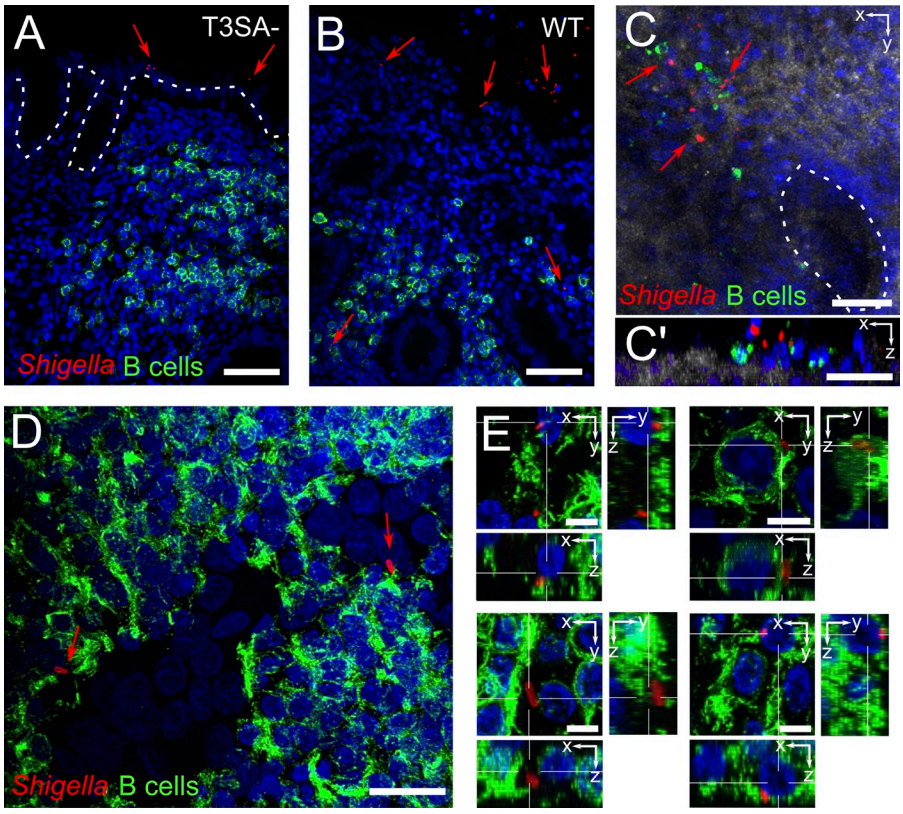

Figure 1. *S. flexneri* interacts with and invades B lymphocytes upon ex vivo infection of human colonic tissue. (A and B) Fluorescence microscopy of histological analysis. T3SA$^-$ bacteria were found attached to the epithelium (A), whereas WT bacteria ruptured the epithelial barrier and got access to underlying tissue (B). (C) Confocal imaging of whole-mount tissue infected with WT bacteria, with top view (C) and orthogonal slice (C'). Reflection is shown in gray and crypts are outlined with a dashed line. (D and E) Confocal imaging of isolated lymph follicles in 150-µm-thick tissue sections, with top view (D) and orthogonal slices (E). Bacteria were stained with an antibody specific for *S. flexneri 5a* (red), B cells with anti-CD20cy (membrane receptor, green), and DAPI nuclei staining is shown in blue. Arrows point to bacteria. Bars: (A and B) 50 µm; (C and C') 40 µm; (D) 20 µm; (E) 5 µm.

acute inflammation contributes to the acquired profile of the adaptive immune response, i.e., by the production of immunosuppressive cytokines and the induction of immune cell death in the lamina propria (LP; Islam et al., 1994; Raqib et al., 1995; Sperandio et al., 2008; Sellge et al., 2010).

However, subversion of host acquired immunity as a consequence of direct interactions between *Shigella* and DCs or T or B lymphocytes has thus far been poorly investigated. Such interactions may take place in colonic isolated lymphoid follicles (ILFs) after *Shigella* crosses the intestinal barrier via M cells located within the follicle-associated epithelium, in the LP, and within mesenteric LNs (Phalipon and Sansonetti, 2007; Sansonetti and Di Santo, 2007). In vitro studies have shown that *Shigella* triggers rapid DC pyroptosis and apoptosis (Edgeworth et al., 2002; Kim et al., 2008). We recently demonstrated that *Shigella* invades activated human CD4$^+$ T cells in vitro and inhibits T cell migration toward a chemoattractant stimulus dependent on the virulence effector IpgD (Konradt et al., 2011). Additionally, *Shigella* impairs T cell dynamics in vivo within the site of adaptive immunity priming, i.e., the LN (Salgado-Pabón et al., 2013). Interactions of *Shigella* with B cells, the lymphocyte population which confers protection against reinfection (Clemens et al., 1986; Oberhelman et al., 1991; Ahmed et al., 1992; Sellge et al., 2010), have not yet been investigated.

B lymphocytes have long been regarded as a simple antibody production unit but are now emerging as key players in adaptive, as well as innate, immune responses (Vaughan et al., 2011). They express TLRs and integrate signals from microbial products with B cell receptor signaling and cognate T cell help during the generation of an antibody response (Ruprecht and Lanzavecchia, 2006; Pone et al., 2010; Rawlings et al., 2012). Different B cell subsets express variable levels of TLRs and can respond differently to their ligands, ranging from sustained proliferation, differentiation, and antibody production to the development of immunosuppressive functions (Hornung et al., 2002; Månsson et al., 2006; Crampton et al., 2010; Lampropoulou et al., 2010; Weller et al., 2012). Considering the close interplay of innate and adaptive pathways in B cell responses and the significant role of B cells in infection and protection, it is not surprising that pathogens have been shown to directly interact with and manipulate B lymphocytes. For instance, certain viruses and parasites induce "diluted" polyclonal antibody responses that confer little protection (Minoprio et al., 1988; Miller et al., 1994; Acosta Rodriguez et al., 2007; Machida et al., 2008). However, few reports have addressed a direct targeting of B lymphocytes by bacterial pathogens (Jendholm et al., 2009; So et al., 2012; Singh et al., 2012).

To investigate the impact of *Shigella* on B lymphocytes, the current study was aimed at characterizing the outcome of *S. flexneri*–B cell cross talks, using ex vivo, in vivo, and in vitro infection models. We demonstrate that *S. flexneri* targets B cells and induces cell death. Besides the cell death induced in *Shigella*-invaded B lymphocytes, we report a mechanism that is independent of invasion or translocation of virulence effectors but dependent on the T3SA virulence factor IpaD.

We provide evidence that bacterial co-signals sensitize B cells to apoptosis and up-regulate *tlr2*, and subsequent binding of IpaD to TLR2 triggers an apoptotic B cell death. These findings reveal a surprising outcome of TLR2 signaling in B cells, adding to the diversity of mechanisms used by *Shigella* to manipulate the adaptive immune response and providing novel insights into the manipulation of B cell responses by bacterial pathogens.

RESULTS

S. flexneri interacts with and occasionally invades B lymphocytes upon ex vivo infection of human colonic tissues

To assess whether or not *S. flexneri* comes into contact with B lymphocytes upon infection, we used an ex vivo infection model of human colonic tissue to mimic the natural environment in which the bacterium triggers its infectious process (Coron et al., 2009). Human colonic tissue pieces were incubated for 6 h with WT, invasive *S. flexneri*, or a noninvasive *S. flexneri* mutant, which is unable to assemble the T3SA (T3SA$^-$ or *mxiD* mutant). Immunohistochemistry of the infected tissues showed that WT but not T3SA$^-$ bacteria breached the epithelial barrier (Fig. 1, A and B). Confocal analysis of fixed whole-mount tissues revealed that WT *S. flexneri* came into contact with LP B cells at sites of epithelial destruction (Fig. 1, C and C′). For confocal analysis deeper within the tissue, we used 150-µm-thick transversal vibratome sections and found WT *S. flexneri* within ILFs both in contact with and intracellular within B cells (Fig. 1, D and E; and Video 1). These findings indicate that invasive *Shigella* interacts with and may invade B lymphocytes upon crossing of the epithelial barrier.

S. flexneri induces human B lymphocyte cell death in vitro

To characterize *Shigella*–B lymphocyte interactions further, we analyzed the outcomes of infection using the CL-01 B cell line, a germinal center B cell line (Cerutti et al., 1998) which we found to express IgA (unpublished data). Cells were infected in vitro at a multiplicity of infection (MOI) of 50 for 30 min before addition of gentamicin to kill all extracellular bacteria. As shown in Fig. 2 A, after infection with WT and T3SA$^-$ bacteria, a significant reduction in cell number was observed at 24 h post infection (p.i.) with WT bacteria only and at 48 h p.i. with both strains, although greater with WT bacteria. As proliferation was similarly reduced upon infection with both strains (unpublished data), the T3SA-specific drop in cell number was not due to an impairment of cell proliferation. Instead, we observed a T3SA-specific induction of cell death, as the percentages of PI$^+$ (propidium iodide–positive) cells were significantly increased upon infection with the WT strain as compared with the T3SA$^-$ strain at 24 and 48 h p.i. (Fig. 2 B). The induction of this T3SA-dependent cell death by WT bacteria is summarized in Fig. 2 C by presenting the reduction of cell number (WT = 0.6× T3SA$^-$) and the induction of PI$^+$ cells (WT = 2× T3SA$^-$) as values normalized to the T3SA$^-$ mutant. To assess if cell death was related to the ability of WT bacteria to invade B cells, CL-01 cells were infected as described above with GFP-expressing T3SA$^-$ and WT bacteria. Invasion was monitored by flow cytometry, focusing on GFP^{high} cells, which have previously been reported to represent cells containing multiple intracellular bacteria (Castro-Eguiluz et al., 2009; Konradt et al.,

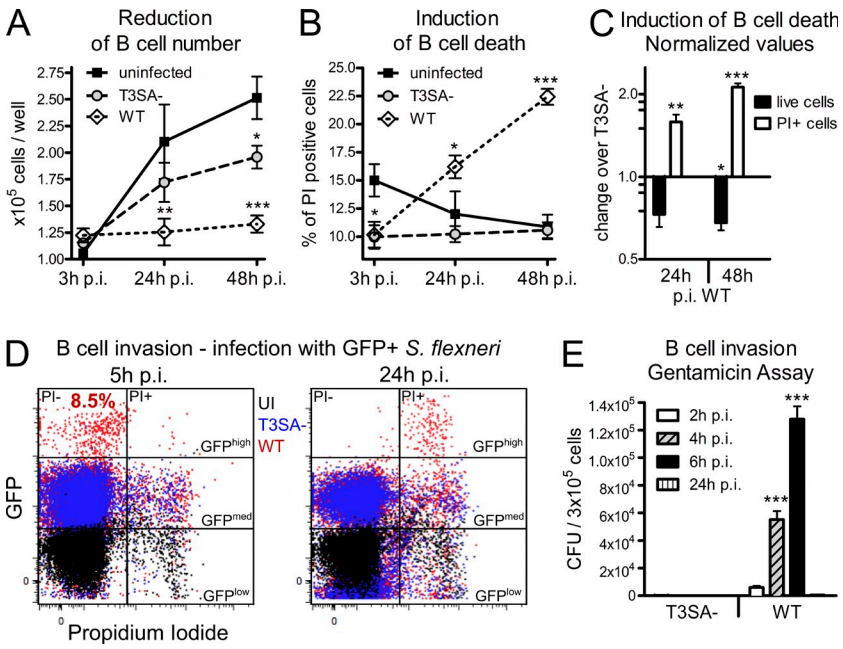

Figure 2. *S. flexneri* induces B cell death dependent on the T3SA in vitro. The human IgA$^+$ CL-01 B cell line was infected for 30 min with WT or T3SA$^-$ bacteria before addition of gentamicin. (A) Count of in vitro–infected human CL-01 B cells over time. Asterisks indicate statistical difference to the uninfected control. (B) Percentages of in vitro–infected PI$^+$ human CL-01 B cells over time. Asterisks indicate statistical difference to the uninfected control. (C) Fold changes of live cell number and percentage of PI$^+$ cells are presented for WT infection over infection with the T3SA$^-$ mutant as normalized values. Asterisks indicate statistical difference to the T3SA$^-$ strain. (D) Flow cytometry analysis of cells infected with GFP-expressing bacteria. GFP^{high} PI$^-$ B cells were detected 5 h p.i. with WT, but not T3SA$^-$ bacteria ($P < 0.001$), representing 8.47 ± 1.1% (mean ± SEM) invaded cells. At 24 h p.i., GFP^{high} cells are PI$^+$. (E) Invasion assay for CL-01 B cells. The number of CFUs per 3 × 10^5 infected cells is presented for WT and T3SA$^-$ bacteria at 2, 4, 6, and 24 h p.i. Three independent experiments were performed in triplicate for A–E and data are presented as mean ± SEM. Statistically significant differences were determined by two-way ANOVA with Bonferroni post-test. *, $P < 0.05$; **, $P < 0.01$; ***, $P < 0.001$.

2011). No GFP^{high} CL-01 B cells were observed upon incubation with T3SA$^-$ bacteria, whereas ∼8.5% of the B cell population was found to be GFP^{high} upon infection with WT bacteria at 5 h p.i. (Fig. 2 D), confirming that invasion was dependent on T3SA activity. At 24 h p.i, the GFP^{high} cells were found to be PI$^+$ (Fig. 2 D), indicating that *Shigella* invasion led to B cell death. Consistently, no intracellular bacteria were detected at 24 h p.i. in the gentamicin invasion assay, whereas the number of intracellular WT bacteria increased at earlier time points, revealing bacterial proliferation inside B cells (Fig. 2 E). Despite only ∼8.5% of the CL-01 cell population being invaded (Fig. 2 D), cell death was induced in ∼15 and 20% of the B cells at 24 and 48 h p.i., respectively (Fig. 2 B). This was neither due to the presence of live, extracellular bacteria, which were killed upon gentamicin treatment, nor to cell-to-cell dissemination given the similar rate of cell death detected upon infection with a nonspreading *icsA* mutant (unpublished data). Altogether, these results indicate that *S. flexneri* triggers T3SA-dependent B lymphocyte death in vitro in both invaded and noninvaded human B cells.

S. flexneri induces murine B lymphocyte death in vivo

A murine model of footpad infection with WT and T3SA$^-$ bacteria was performed as previously described (Salgado-Pabón et al., 2013) to assess the potential induction of B cell death by *S. flexneri* in vivo. Consistent with the priming of an immune response, the total cell number increased in the draining LNs of infected mice as compared with uninfected ones, with no difference between WT and T3SA$^-$ bacteria (Fig. 3 A). In contrast, despite an increase of the percentage of CD19$^+$ B lymphocytes upon infection, the B cell compartment was significantly reduced in LNs upon infection with WT bacteria as compared with the T3SA$^-$ strain (Fig. 3 B). Accordingly, WT bacteria induced higher B cell death than the T3SA$^-$ strain (Fig. 3 C). Differences in the percentages of CD4$^+$ T lymphocytes inversely correlated with the percentages of CD19$^+$ cells, indicating that the reduction of the cellular compartment was specific to B lymphocytes (Fig. 3 D). Similar bacterial counts were detected in the LNs after infection with either *Shigella* strain (Fig. 3 E). *S. flexneri* thus causes murine B cell death in vivo in a T3SA-dependent manner.

S. flexneri–induced human B cell death is dependent on the T3SA virulence factor IpaD

To identify the virulence factors responsible for the induction of human B cell death, CL-01 cells were infected with a panel of *S. flexneri* mutants. To discriminate between varying types of translocated effectors (Parsot, 2009), we tested the contribution of effectors whose expression is dependent on the transcriptional factor MxiE, using a *mxiE* mutant, as well as those binding the chaperone Spa15, by using a *spa15* mutant. Neither mutant was impaired in its ability to induce CL-01 B cell death, as each exhibited a profile similar to that of WT bacteria both for cell number and percentage of PI$^+$ cells (Fig. 4 A). We thus assessed the contribution of the virulence factors IpaC and IpaD, which are required for pore formation, translocation of T3SA effectors, and invasion of host cells (Ménard et al., 1993; Blocker et al., 1999; Parsot, 2009). Surprisingly, a different outcome was observed with the two noninvasive *ipaC* and *ipaD* mutants. CL-01 B cell death was induced by the *ipaC* mutant, but not by the *ipaD* mutant, which exhibited cell numbers and percentages of PI$^+$ cells comparable to that of T3SA$^-$ bacteria. The WT bacteria-induced cell death phenotype was observed using a complemented *ipaD*/pIpaD strain (Fig. 4 A). These results indicate that IpaD, which is located at the tip of the T3SA needle (Espina et al., 2006; Sani

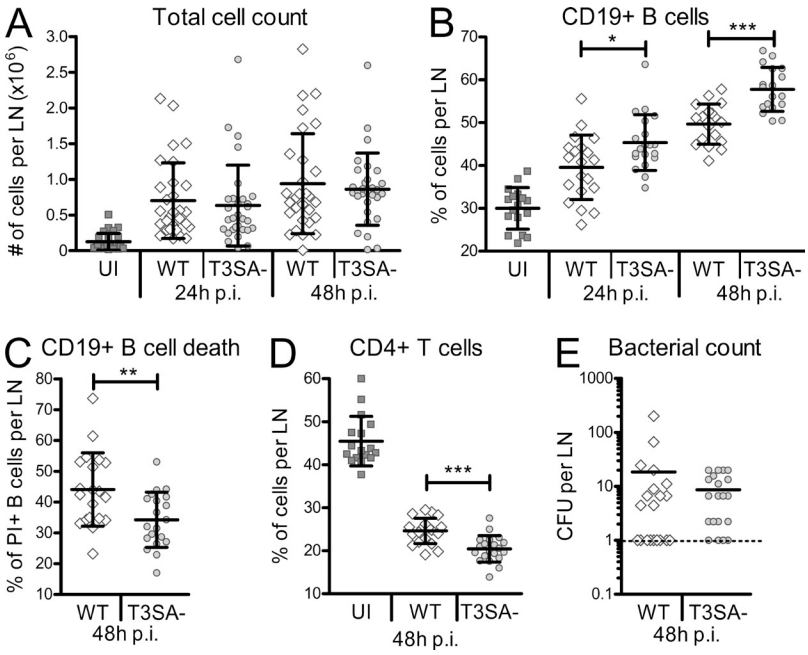

Figure 3. *S. flexneri* induces B cell death dependent on the T3SA in vivo. (A) Total cell count in murine LNs after footpad infection with *S. flexneri*. Cells were counted 24 and 48 h after WT and T3SA$^-$ infection. (B) Percentages of CD19$^+$ B cells in murine popliteal LNs 24 and 48 h after footpad infection. (C) Percentages of PI$^+$ CD19$^+$ B cells in murine popliteal LNs 48 h after footpad infection. (D) Percentages of CD4$^+$ T cells in murine popliteal LNs 48 h after footpad infection. (E) Number of CFUs for WT and T3SA$^-$ bacteria in murine LNs 48 h after footpad infection. Two independent experiments with each 5 mice per group (10 LNs) were performed and data are presented as mean ± SEM. Asterisks indicate statistical significant differences between WT and T3SA$^-$, determined by Mann-Whitney Student's *t* test. *, P < 0.05; **, P < 0.01; ***, P < 0.001.

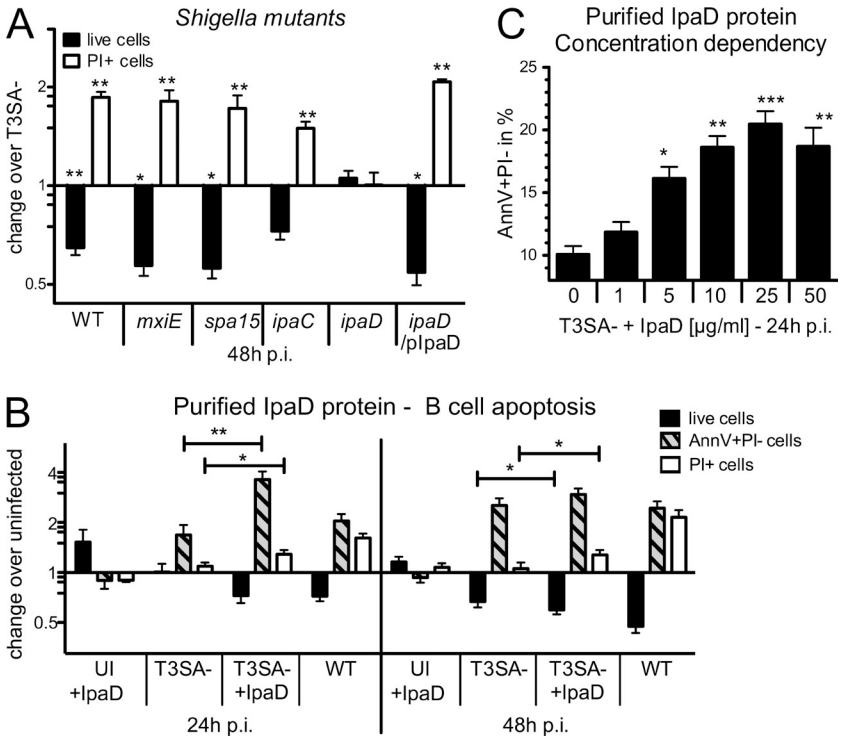

Figure 4. *S. flexneri*–induced B cell apoptosis is dependent on the virulence factor IpaD. (A) In vitro infections of the CL-01 B cell line with WT, *mxiE*, *spa15*, *ipaC*, *ipaD*, and complemented *ipaD* (*ipaD*/pIpaD) *S. flexneri* strains. Fold changes in cell number and percentages of PI^+ cells are presented for infection with each strain over infection with the $T3SA^-$ strain. Asterisks indicate statistical differences to $T3SA^-$ bacteria. (B) CL-01 cell number and percentages of $AnnV^+PI^-$ (Annexin V^+PI^-) and PI^+ populations at 24 and 48 h p.i. for uninfected cells incubated with 25 µg/ml His-tagged IpaD protein (UI + IpaD), $T3SA^-$-infected cells, cells infected with $T3SA^-$ and co-incubated with IpaD ($T3SA^-$ + IpaD), and WT infected cells. Data are presented as fold change over the uninfected control. Asterisks indicate statistically significant differences between $T3SA^-$ and $T3SA^-$ + IpaD. (C) Percentages of apoptotic $AnnV^+PI^-$ cells after 24 h of co-incubation with $T3SA^-$ and different concentrations of IpaD. Asterisks indicate statistical differences to $T3SA^-$ bacteria alone. Three independent experiments were performed in triplicate for each condition/bacterial strain and data are presented as mean ± SEM. Statistically significant differences were determined by one-way (C) or two-way (A and B) ANOVA with Bonferroni post-test. *, $P < 0.05$; **, $P < 0.01$; ***, $P < 0.001$.

et al., 2007; Epler et al., 2012), is required to trigger CL-01 B cell death independently of its role in translocation of T3SA effectors and that IpaD-mediated signals may account for the cell death observed in noninvaded CL-01 B lymphocytes.

IpaD induces human B lymphocyte apoptosis in the presence of bacterial co-signals

Given the above results, we hypothesized that exposure of cells to IpaD might be sufficient to trigger B cell death. To test this hypothesis, CL-01 B cells were incubated with purified His-tagged IpaD. To analyze the nature of cell death observed (necrosis versus apoptosis), analysis of Annexin V^+PI^- ($AnnV^+PI^-$) apoptotic B cells was included in the measurement. After 24 and 48 h of exposure, no differences in cell number or induction of cell death ($AnnV^+PI^-$ or PI^+ cells) were observed as compared with untreated cells (Fig. 4 B), indicating that IpaD alone did not trigger B cell death. Requirement for the presence of bacterial co-signals was then assessed by incubating CL-01 cells with $T3SA^-$ bacteria and medium containing the IpaD protein ($T3SA^-$ + IpaD). The $T3SA^-$ mutant alone was able to induce an increase in the $AnnV^+PI^-$ population at 24 and 48 h p.i., along with the slight reduction in cell number previously observed at 48 h p.i. (Fig. 4 B). However, co-incubation of the $T3SA^-$ mutant with IpaD led to a significant increase of the apoptotic $AnnV^+PI^-$ population at 24 h p.i., accompanied by a significant induction of PI^+ cells and reduction of live cell number at 48 h p.i. in comparison to incubation with $T3SA^-$ alone (Fig. 4 B). Induction of $AnnV^+PI^-$ B cells at 24 h p.i. was shown to be dependent on the concentration of IpaD, with a maximum of apoptotic cells reached at 25 µg/ml (Fig. 4 C), the concentration used in all other experiments unless otherwise indicated. This increase in apoptotic cell death was specific to IpaD, as His-tagged MxiH, another component of the T3SA, did not induce CL-01 cell death when added with $T3SA^-$ bacteria (unpublished data).

In an attempt to identify the microbial products acting as co-signals, we generated bacterial lysates of the *ipaD* strain by killing bacteria by gentamicin treatment, sonication, or heat before their addition to B cells. Additionally, we tested a panel of pathogen-associated molecular patterns (PAMPs). As shown in Fig. 5 A, LPS, PGN, CpG, or combinations of these products did not provide the required co-signals to induce apoptotic $AnnV^+PI^-$ cells at 24 h after incubation in the presence of IpaD. Surprisingly, whereas live or gentamicin-treated *ipaD* lysates provided the co-signals, *ipaD* lysates generated by heat killing or sonication did not. Altogether, these results indicate that *S. flexneri* induces B lymphocyte apoptosis through the combined action of IpaD and bacterial co-signals and does so in the absence of invasion or translocation of effectors.

Bacterial co-signals sensitize human B lymphocytes to IpaD-mediated mitochondrial apoptosis

A balance between a complex network of signaling pathways involving NF-κB and pro- and anti-apoptotic Bcl-2 proteins drives B cells toward either survival or death (Graves et al., 2004; Sen, 2006). To investigate the apoptotic pathway leading to IpaD-mediated B cell death, we conducted a protein-based apoptosis array, which revealed that apoptosis was mainly mediated by mitochondrial factors (Table S1). During necrotic and apoptotic death of epithelial cells induced by *Shigella* infection, the loss of mitochondrial membrane potential (MMP) has previously been reported (Koterski et al., 2005; Carneiro

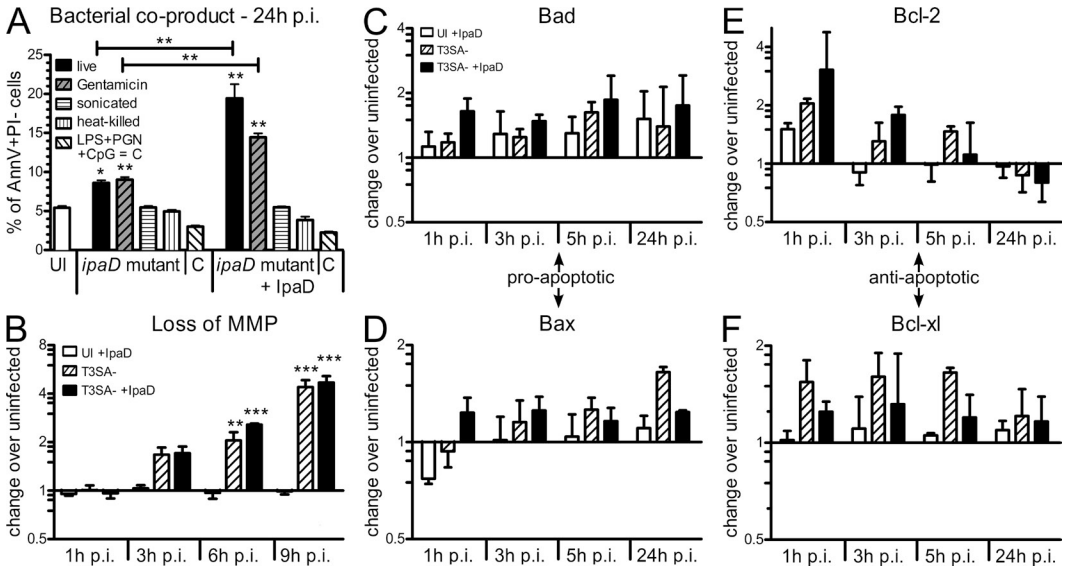

Figure 5. Bacterial co-signals sensitize human B lymphocytes to IpaD–mediated mitochondrial apoptosis. (A) Apoptotic CL-01 B cells after incubation for 24 h with live, gentamicin-treated, sonicated, or heat-killed *ipaD* bacteria or a cocktail of LPS, PGN, and CpG (C). Percentages of AnnV$^+$PI$^-$ cells are shown, in the presence (+IpaD) or absence of IpaD. Asterisks indicate statistical differences to the uninfected control (on column) or between conditions (indicated by bars) determined by one-way ANOVA with Bonferroni post-test. *, $P < 0.05$; **, $P < 0.01$. (B) Loss of MMP as assessed by flow cytometry with the fluorescent probe JC-1. Fold changes in the percentage of cells that lost MMP are presented for T3SA$^-$ and T3SA$^-$ + IpaD over the uninfected control. Asterisks indicate statistical differences to the uninfected control determined by two-way ANOVA with Bonferroni post-test. **, $P < 0.01$; ***, $P < 0.001$. (C–F) Dynamic regulation of mitochondrial pro- and anti-apoptotic proteins over time. Protein amounts were assessed by Western blot at 1, 3, 5, and 24 h p.i., and are presented as fold change over the uninfected control for IpaD alone, T3SA$^-$, and T3SA$^-$ + IpaD after normalization to actin. (C and D) Protein amounts of pro-apoptotic Bad (C) and Bax (D). (E and F) Protein amounts of anti-apoptotic Bcl-2 (E) and Bcl-x_L (F). All data are presented as mean ± SEM for three independent experiments.

et al., 2009; Lembo-Fazio et al., 2011). Therefore, we assessed the loss of MMP by flow cytometry with the mitochondrial probe JC1. Incubation of B cells with T3SA$^-$ and T3SA$^-$ + IpaD induced an increasing loss of MMP over time starting from as early as 3 h p.i. (Fig. 5 B). Based on these results, the dynamic regulation of mitochondrial pro- and anti-apoptotic proteins during infection was assessed by quantification of protein amounts at 1, 3, 5, and 24 h p.i. As compared with the uninfected control, the T3SA$^-$ strain alone up-regulated the pro-apoptotic proteins Bad and Bax (Fig. 5, C and D) but also anti-apoptotic Bcl-x_L (Fig. 5 F). Anti-apoptotic Bcl-2 was up-regulated at early time points but slightly down-regulated at 24 h p.i. (Fig. 5 E). IpaD alone and in combination with T3SA$^-$ bacteria only led to nonsignificant differences in the amounts of pro- and anti-apoptotic proteins when compared with uninfected cells or cells incubated with the T3SA$^-$ alone, respectively (Fig. 5, C–F). In summary, our results suggest that bacterial co-signals, while not inducing cell death (Fig. 2, B and C), render B lymphocytes prone to die. It is likely that modulation of pro- and anti-apoptotic mitochondrial proteins and the loss of MMP further promote IpaD-mediated triggering of apoptosis.

IpaD binds to and is internalized by human CL-01 B lymphocytes

As extracellular exposure to IpaD in the presence of bacterial co-signals triggers B cell apoptosis, we assessed IpaD binding to CL-01 B cells. His-tagged IpaD and MxiH were coupled to Alexa Fluor 488 (AF488) and incubated with B cells in the presence of T3SA$^-$ bacteria for 2 h at 37°C. Whereas no fluorescence was detected with AF488-MxiH, labeling of B cells was detected upon incubation with AF488-IpaD (Fig. 6 A). As illustrated in Fig. 6 A, the detection of AF488-IpaD in orthogonal slices suggested a specific interaction of IpaD with B cells. To further assess IpaD–CL-01 association, we compared the interaction of AF488-IpaD with these cells in different conditions by measuring relative mean AF488 fluorescence intensities within 15-µm-diameter spheres centered on B cell nuclei. In agreement with results from Fig. 6 A, the relative mean intensity was significantly higher upon incubation at 37°C with IpaD as compared with MxiH (Fig. 6 B). AF488-IpaD relative mean intensity was significantly increased upon incubation at 37°C as compared with 4°C (Fig. 6 B) and with time (Fig. 6 C), suggesting an active internalization process. Indeed, ∼50 and 75% of IpaD bound to B cells at 4°C was internalized after 30 and 60 min incubation at 37°C, respectively (Fig. 6 D). It is noteworthy that the presence of T3SA$^-$ bacteria significantly reduced IpaD association after 30 min of incubation with the cells, while significantly increasing it at 24 h after incubation (unpublished data). These findings show that exposure of IpaD to B cells results in its binding and internalization and suggests the existence of a specific interaction partner for IpaD at the B cell surface.

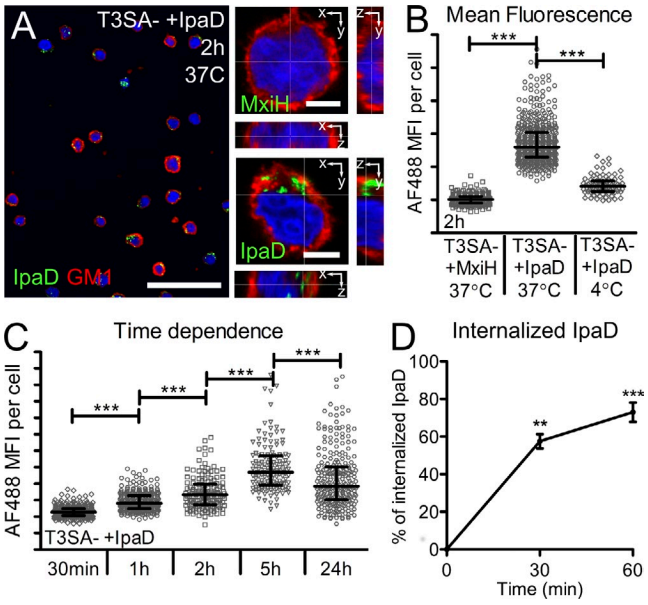

Figure 6. IpaD binds to human CL-01 B lymphocytes and is internalized. (A) Confocal images of CL-01 B cells incubated with T3SA⁻ bacteria and IpaD or MxiH coupled to Alexa Fluor 488. An overview image (bar, 50 µm) is presented alongside single confocal slices of B cells (bars, 5 µm) after 2 h of incubation at 37°C. Cells were co-stained for GM1 (red, membrane) and DAPI (blue, nuclei). (B and C) Quantification of the AF488 mean fluorescence intensity (MFI) in a 15-µm radius around the center of the nuclei. (B) MFI of IpaD after co-incubation with T3SA⁻ for 2 h at 37°C. Values are compared with the MxiH control protein and to incubation at 4°C. (C) Time dependence of the MFI measured for IpaD. Cells were incubated with IpaD for different times at 37°C in the presence of T3SA⁻ bacteria. A minimum of 100 cells were analyzed for each condition for B and C. Data are presented as median ± interquartile range for one representative experiment and statistically significant differences were determined by Kruskal-Wallis test with Dunn's post-test. ***, $P < 0.0001$. (D) IpaD internalization. Cells were incubated with fluorescent AF488-IpaD for 1 h at 4°C (time 0), and unbound AF488-IpaD was washed before incubation at 37°C for 30 min or 1 h. At each time point, IpaD bound to the cell surface was detected by flow cytometry using an anti-IpaD polyclonal serum, and a secondary antibody coupled to Alexa Fluor 647. Data are presented as mean ± SEM for three independent experiments and statistically significant differences to time 0 were determined by one-way ANOVA with Bonferroni post-test. **, $P < 0.01$; ***, $P < 0.001$.

IpaD induces B cell apoptosis via interaction with TLR2

IpaD shares structural and functional similarities with the *Yersinia* effector LcrV that has been shown to signal in a TLR2-dependent manner (Sing et al., 2002; Espina et al., 2007). Induction of apoptosis by a TLR2-mediated signaling pathway has been reported in different cell types (Aliprantis et al., 1999); however, to our knowledge, no information is available regarding B lymphocytes. Based on the similarity between IpaD and LcrV and the need of bacterial co-signals for the induction of B cell death, we aimed at investigating the involvement of TLRs in the signaling pathways resulting in human B cell death. Therefore, we first assessed basal levels of mRNA expression of different *tlr* genes by quantitative RT-PCR in the CL-01 B cell line. *tlr2* was expressed at low levels as compared with *tlr1*, *7*, and *10* (highly expressed) and *tlr3*, *6*, and *9* (expressed at intermediate levels). Expression of *tlr4*, *5*, and *8* was not detected (Fig. 7 A). Then, we assessed *tlr* expression upon incubation of cells with T3SA⁻, T3SA⁻ + IpaD, or WT bacteria for 24 h. Interestingly, only *tlr2* showed significant changes in its expression levels upon infection with its mRNA levels significantly up-regulated upon incubation with the T3SA⁻ strain (eightfold change, Fig. 7 B). Whereas IpaD alone had no effect, a combination of IpaD and T3SA⁻ bacteria or infection with WT bacteria led to a significant decrease in *tlr2* as compared with T3SA⁻ bacteria alone (Fig. 7 B). Bacterial co-signals thus lead to up-regulation of *tlr2*.

To assess the involvement of TLR2, and its described heterodimer partners, in the induction of apoptotic AnnV⁺PI⁻ cells, cells were transfected with siRNA pools against TLR1, 2, 6, and 10 and incubated with IpaD in the presence of the T3SA⁻ strain. As shown in Fig. 7 C, a significant decrease in the percentage of AnnV⁺PI⁻ cells occurred in CL-01 B cells transfected with TLR1- or TLR2-targeting siRNA as compared with cells transfected with nontargeting siRNA. Decreasing *tlr6* or *tlr10* levels had no impact on the amount of apoptotic cells. To test whether or not IpaD could indeed signal via TLR2-1, we assessed binding of IpaD in the presence of blocking antibodies. Based on the observed up-regulation of *tlr2* at 24 h p.i. with T3SA⁻ bacteria (Fig. 7 B), we preincubated cells for 22 h with the T3SA⁻ strain, added TLR1 and TLR2 blocking antibodies for 1 h, and subsequently added AF488-IpaD for 2 h. As compared with untreated cells, a significant decrease in IpaD binding/internalization was measured in the presence of both blocking antibodies (Fig. 7 D). Similarly, we observed a significant decrease in the amount of AnnV⁺PI⁻ cells in cells treated with the TLR2 (but not TLR1) blocking antibody before addition of IpaD for 6 h (Fig. 7 E). Preincubation of IpaD with an anti-IpaD antibody displayed a similar phenotype (Fig. 7 E). TLR2 and TLR1 are thus involved in the induction of IpaD-mediated apoptosis.

Based on these results, we aimed at investigating TLR signaling upon infection in CL-01 B cells. Activation of the NF-κB signaling pathway was assessed by measuring IκBα amounts using Western blot analysis. Whereas no change in the amount of IκBα occurred with IpaD alone, the intensity of the IκBα band decreased, and an additional lower band was detected for cells incubated with T3SA⁻, T3SA⁻ + IpaD, and WT *Shigella* (Fig. 7 F). The TLR2 "death pathway" has been reported to bifurcate from NF-κB activation at the level of MyD88 via a pathway involving FADD (Fas-associated death domain protein; Aliprantis et al., 2000). We also assessed FADD protein amounts by Western blot analysis. In contrast to the NF-κB pathway, which was similarly activated in B cells under all conditions that included incubation with bacteria, we detected higher amounts of FADD for B cells incubated with T3SA⁻ + IpaD or WT bacteria, but not for B cells incubated with the T3SA⁻ mutant alone (Fig. 7 F). We thus observed changes in the TLR2 "death pathway" dependent on IpaD.

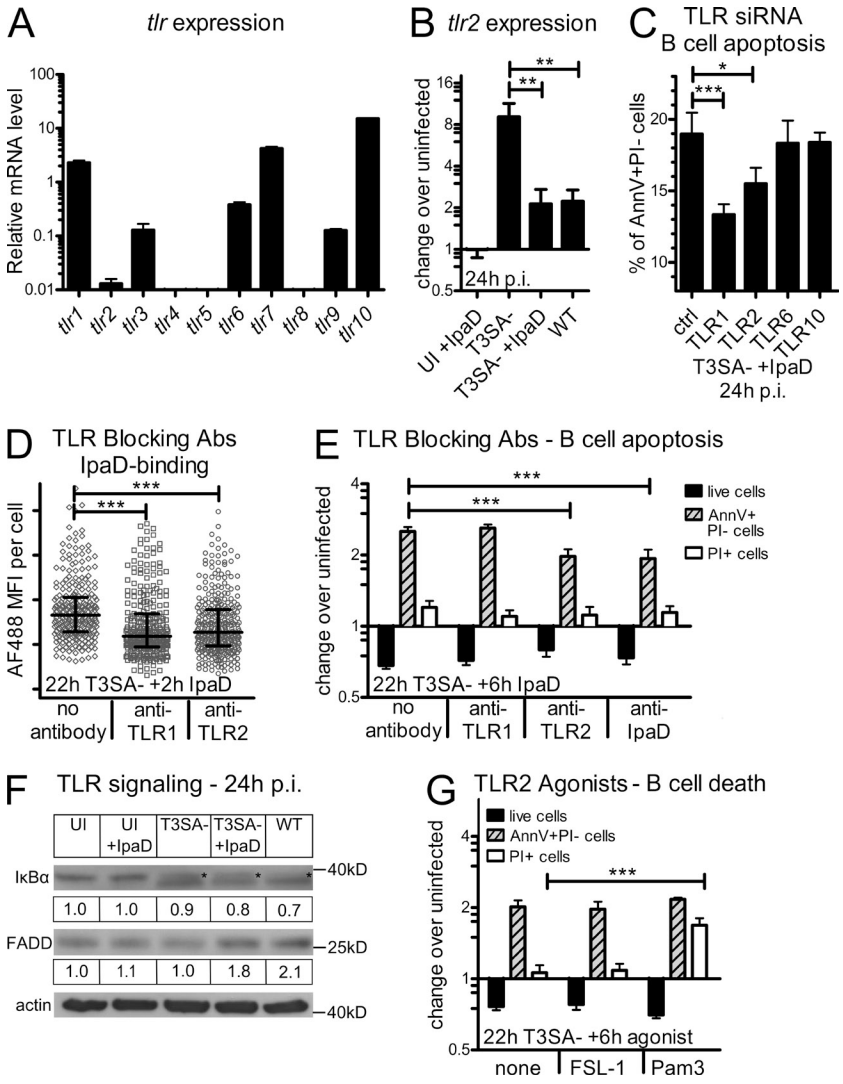

Figure 7. IpaD induces B cell apoptosis via interaction with TLR2. (A) Relative TLR mRNA expression levels in the CL-01 B cell line as assessed by quantitative RT-PCR. (B) TLR2 mRNA expression levels after 24 h of incubation with IpaD alone, T3SA$^-$, WT, or T3SA$^-$ + IpaD. mRNA levels are presented as fold change over the uninfected control. Asterisks indicate a statistical difference between T3SA$^-$ and T3SA$^-$ + IpaD/WT determined by one-way ANOVA with Bonferroni post-test. **, $P < 0.01$. (C) Apoptotic CL-01 B cells after transfection with TLR-targeting siRNA pools. Transfection was performed 24 h before incubation with T3SA$^-$ + IpaD and percentages of AnnV$^+$PI$^-$ cells are presented 24 h p.i. Asterisks indicate statistical differences to the nontargeting control siRNA pool determined by one-way ANOVA with Bonferroni post-test. *, $P < 0.05$; ***, $P < 0.001$. (D) IpaD binding to B cells in the presence of TLR1 and 2 blocking antibodies. IpaD coupled to Alexa Fluor 488 was added for 2 h to cells preincubated with the T3SA$^-$ mutant for 22 h. The blocking antibodies were added 1 h before IpaD addition. Asterisks indicate statistical differences to the control without antibody determined by Kruskal-Wallis test with Dunn's post-test. ***, $P < 0.0001$. (E) B cell death in the presence of TLR1 and 2 blocking antibodies or an antibody against IpaD. IpaD was added for 6 h to cells preincubated with the T3SA$^-$ mutant for 22 h. The TLR blocking antibodies were added to the cells, and the anti-IpaD antibody to the IpaD solution, 1 h before IpaD addition to the cells. Live cell numbers and percentages of AnnV$^+$PI$^-$ and PI$^+$ cells are presented as fold changes over the uninfected control. Asterisks indicate statistical differences to the control without antibody determined by two-way ANOVA with Bonferroni post-test. ***, $P < 0.001$. (F) TLR signaling at 24 h p.i. as assessed by Western blot analysis. Protein amounts of IκBα were assessed as an indicator for NF-κB activation and FADD as an indicator of the TLR2 death pathway. Pictures of the blots and the correspondent fold change over the uninfected control after normalization to actin are shown for both proteins. (G) Induction of B cell death by a TLR2 agonist. The TLR2-6 agonist FSL-1 and the TLR2-1 agonist Pam3CSK4 were added for 6 h to cells preincubated with the T3SA$^-$ mutant for 22 h. Live cell numbers and percentages of AnnV$^+$PI$^-$ and PI$^+$ cells are presented as fold changes over the uninfected control. Asterisks indicate statistical differences to T3SA$^-$ bacteria alone determined by two-way ANOVA with Bonferroni post-test. ***, $P < 0.001$. Data are presented as mean ± SEM (A–C, E, and G) and as median ± interquartile range in D. Three independent experiments were performed in triplicate for A–C, E, and G, and one representative out of two independent experiments is shown in D and F.

Finally, we assessed the ability of known TLR2 agonists to induce B cell death in the CL-01 B cell line. As shown in Fig. 7 G, the TLR2-1 agonist Pam3, but not the TLR2-6 agonist FSL-1, led to a significant increase in PI$^+$ B cells in the presence of T3SA$^-$ as compared with untreated cells. These results show that CL-01 B cells are indeed sensitive to TLR2-1–induced cell death. Altogether, these data indicate that bacterial co-signals promote IpaD–TLR2 interaction by up-regulating *tlr2*, and that IpaD induces B cell death via TLR2-signaling.

IpaD is a TLR2 agonist

To formally demonstrate that IpaD signals via TLR2, we used a cell-based reporter system previously described (Burger-Kentischer et al., 2010). The reporter system is based on NIH3T3 cells stably transfected with the NF-κB–inducible reporter gene SEAP (secreted alkaline phosphatase) together with the corresponding combinations of human TLRs. The amount of SEAP upon TLR induction can be compared in cell supernatants by addition of its substrate pNPP and measurement of the product OD at 405 nm. As shown in Fig. 8 A, a concentration-dependent induction of the TLR2-1 and TLR2-6 reporter cell lines occurred when adding IpaD. At a concentration of 5 µg/ml IpaD, the activation levels of TLR2-1 and TLR2-6 were comparable to 1 µg/ml of the positive controls Pam3CSK4 and FSL-1, respectively (Fig. 8, B and C). These results demonstrate that

IpaD binds to and induces activation of the human TLR2 signaling pathway.

S. flexneri interacts with B lymphocytes and induces B cell apoptosis upon natural infection in humans

To assess *Shigella*-induced B cell apoptosis upon natural infection, we investigated *S. flexneri*–B lymphocyte interactions in patients diagnosed with shigellosis. Rectal biopsies from *Shigella*-infected patients presenting severe symptoms within 3–4 d of the onset of disease were chosen for immunohistochemistry analysis. As shown in Fig. 9, *S. flexneri* detected by using an anti-IpaD antibody was found in ILFs and in contact with apoptotic B lymphocytes, identified as TUNEL-positive cells. These findings suggest that *S. flexneri*–mediated B cell apoptosis indeed occurs in naturally infected patients.

DISCUSSION

In this study, we provide new insights into the diversity of mechanisms used by *Shigella* to dampen host adaptive immune responses. We report a T3SA-dependent targeting of human B lymphocytes by *S. flexneri* and induction of cell death. Besides cell death occurring in invaded cells, we show induction of B cell apoptosis that is independent of invasion and translocation of virulence effectors but dependent on interaction of the needle tip protein IpaD with TLR2.

Our results show that *S. flexneri* directly interacts with and invades human B lymphocytes in a T3SA-dependent manner. Previous studies on the intracellular presence of facultative intracellular bacteria in B lymphocytes mainly focused on receptor-mediated internalization processes (Menon et al., 2003; Jendholm et al., 2009; Castro-Eguiluz et al., 2009; Goenka et al., 2012). Thus far, the contribution of the T3SA, indicating an active invasion process by the bacterium, has only been shown for *Salmonella* (Souwer et al., 2009). Susceptibility of B lymphocytes to T3SA-mediated *S. flexneri* invasion was low compared with invasion rates previously reported for T lymphocytes (Konradt et al., 2011).

We provide evidence that *S. flexneri* triggers cell death of CL-01 B cells in vitro and of murine B lymphocytes in vivo and that the induction of cell death is mediated by the virulence factor IpaD. Cell death of B lymphocytes in vitro has previously been described for *Listeria monocytogenes*, *Francisella tularensis*, *Neisseria gonorrhea*, and *Helicobacter pylori* (Menon et al., 2003; Pantelic et al., 2005; Singh et al., 2006; Krocova et al., 2008; Zivna et al., 2010). In the case of *L. monocytogenes*, cytotoxicity was shown to be dependent on the virulence

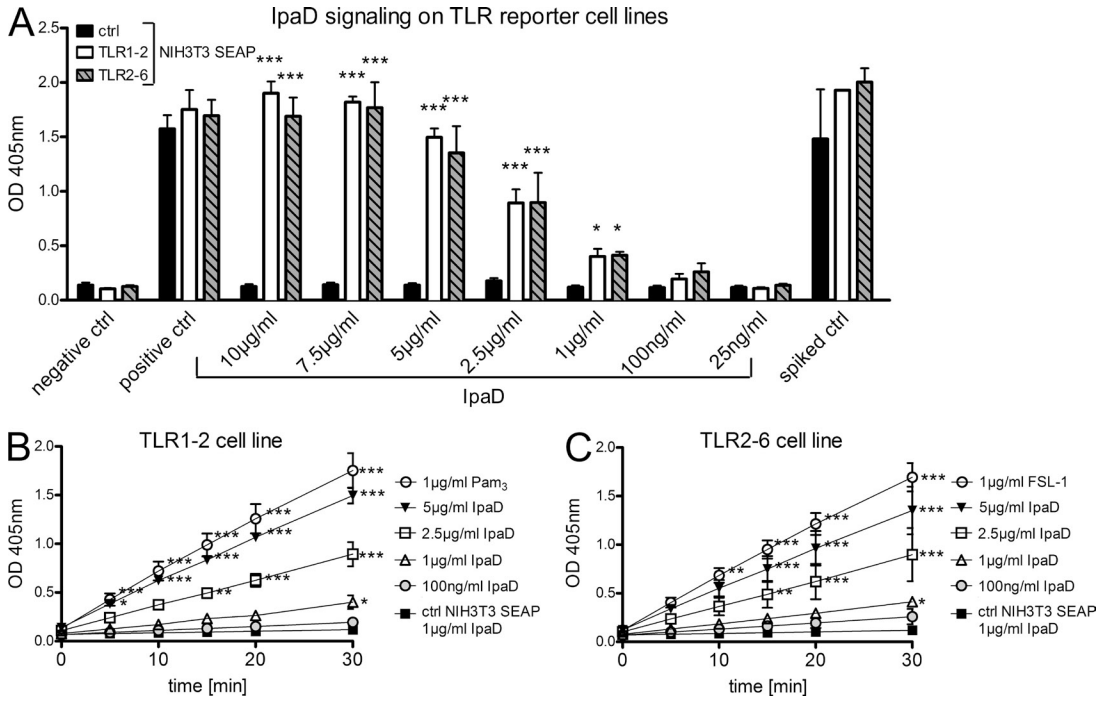

Figure 8. IpaD acts as a TLR2 agonist. The reporter system is based on NIH3T3 cells stably transfected with the NF-κB–inducible reporter gene SEAP together with the corresponding combinations of human TLRs. The amount of SEAP upon TLR induction can be compared in cell supernatants by addition of its substrate pNPP and measurement of the product OD at 405 nm. (A) OD at 405 nm 30 min after substrate incubation with supernatants from treated cells. Cells were treated for 18 h with indicated concentrations of IpaD in comparison to negative, positive, and spiked controls. The TLR2-1 and 2–6 reporter cell lines are shown in comparison to the control SEAP cell line without TLRs. (B) Induction of the TLR2-1 reporter cell line. The OD at 405 nm is presented over time for selected concentrations of IpaD in comparison to positive (Pam3CSK4) and negative (NIH3T3 control cell line) controls. (C) Induction of the TLR2-6 reporter cell line. The OD at 405nm is presented over time for selected concentrations of IpaD in comparison to positive (FSL-1) and negative (NIH3T3 control cell line) controls. Two independent experiments were performed in duplicate and all data are presented as mean ± SEM. Statistically significant differences to the control SEAP cell line were determined by two-way ANOVA with Bonferroni post-test. *, $P < 0.05$; **, $P < 0.01$; ***, $P < 0.001$.

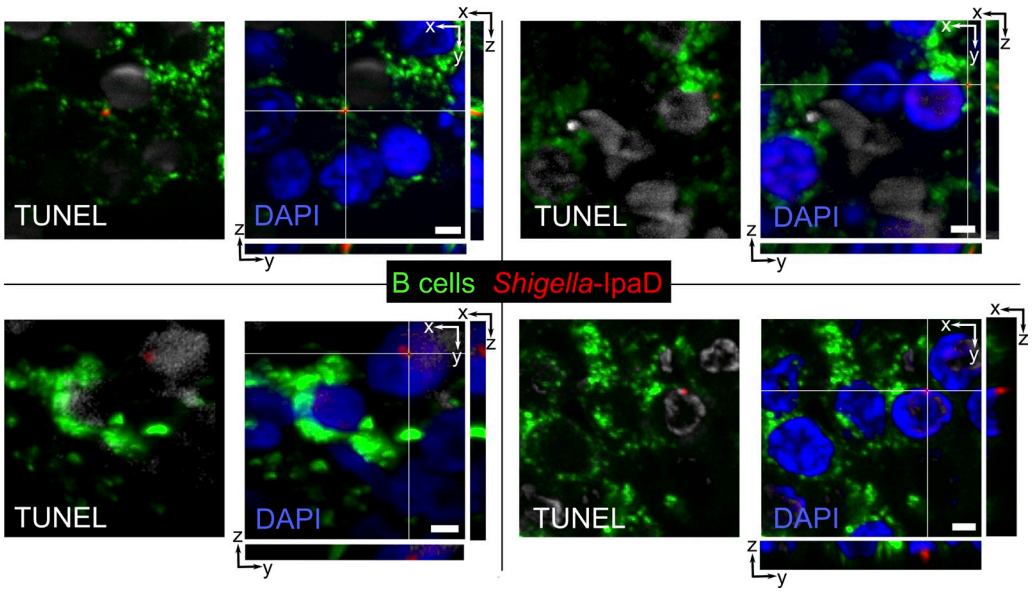

Figure 9. *S. flexneri* interacts with B lymphocytes and induces B cell apoptosis upon natural infection. Representative fluorescence microscopy images of ILFs in colonic biopsy tissue slides from two patients presenting severe shigellosis are shown. Bacteria were stained with an antibody against IpaD (red), B cells with anti-CD20cy (green), and apoptotic cells with a TUNEL kit (gray). Orthogonal slices are shown for each confocal image. Bars, 2 µm.

effector listeriolysin O (LLO), a pore-forming protein causing membrane damage (Bhunia and Feng, 1999; Menon et al., 2003). The occurrence of cell death in vivo has not been addressed in such studies, and the participating virulence effectors, with the exception of LLO, have not been identified.

S. flexneri–induced B cell death occurred both in invaded and noninvaded cells. We recently reported an injection-only–based mechanism for *Shigella*-induced impairment of T cell migration (Konradt et al., 2011). However, this mechanism does not account for *Shigella*-induced cell death of noninvaded B lymphocytes, as the *ipa*C mutant, which is unable to translocate virulence effectors into the host cytoplasm, was able to induce B cell death. In contrast, we observed a novel invasion- and injection-independent mechanism, which is dependent on exposure of B cells to the virulence factor IpaD. This mechanism was revealed by the inability of the *ipaD* mutant to induce B cell death and by the observation that the addition of soluble His-tagged IpaD to cells incubated with T3SA$^-$ bacteria is sufficient to induce B cell apoptosis. IpaD is a hydrophilic coiled-coil protein that, together with IpaB, is located at the needle tip of the *Shigella* T3SA (Ménard et al., 1994; Espina et al., 2006; Sani et al., 2007; Johnson et al., 2007). Needle-tip proteins of other T3SA-bearing bacteria include EspA, LcrV, PcrV, BipD, and SipD, for EPEC (enteropathogenic *Escherichia Coli*), *Yersinia* spp., *Pseudomonas aeruginosa*, *Burkholderia pseudomallei*, and *Salmonella* spp, respectively (Johnson et al., 2007; Espina et al., 2007; Moraes et al., 2008; Lunelli et al., 2011). Although these proteins exhibit no primary sequence similarities, they possess similar structural and functional features and have been described to act as a "plug" for the T3SA (Espina et al., 2007; Sani et al., 2007; Moraes et al., 2008). Soluble *Yersinia* LcrV has also been described to accumulate in serum of infected mice early during the onset of disease (Flashner et al., 2010). Whether or not IpaD is secreted by *S. flexneri* during an infection in vivo is unfortunately still unknown.

Similarly to *Yersinia* LcrV, which has been shown to exploit TLR2 signaling in macrophages (Sing et al., 2002), we provide evidence that IpaD interacts with TLR2 on B cells and subsequently mediates B cell apoptosis. To our knowledge, we hereby provide the first evidence that TLR2 signaling can lead to apoptosis of B lymphocytes, a cell type which has thus far been considered to integrate TLR signals mainly for activation and differentiation (Ruprecht and Lanzavecchia, 2006; Pone et al., 2010; Rawlings et al., 2012). Whereas previous reports have shown that TLR2 activation by bacterial lipoproteins can lead to activation, as well as apoptosis, these studies were conducted mostly with monocytes (Aliprantis et al., 1999, 2000). Interestingly, the induction of IpaD-mediated cell death was impaired by blocking TLR2 and TLR1, but not TLR6, indicating that IpaD death signals occur via the TLR2-1 heterodimer. Consistently, a TLR2-1 agonist, though not a TLR2-6 agonist, induced cell death in the CL-01 B cell line. However, IpaD induced comparable levels of activation in TLR2-1 and TLR2-6 reporter cell lines, indicating that activation signals can occur via both heterodimers. The identification of the virulence factor IpaD as ligand for the TLR2 "death pathway" on human B cells thus opens the possibility for further studies addressing the diversity of ligands and their molecular interactions with TLR2 and its heterodimer partners in activation and apoptosis of immune cells.

Intriguingly, IpaD-dependent B cell apoptosis was only triggered in the presence of bacterial co-signals. None of the common PAMPs known to induce responses in B lymphocytes

acted as co-signals. The observation that sonicated or heat-killed bacteria also lost their co-signal activity as compared with live or gentamicin-treated bacteria suggests that these microbial products are unstable, have to be presented on intact bacteria, or require a particular pathway to be properly delivered to B cells. Identification of the co-signals thus provides a challenging, still ongoing endeavor. However, our results have elucidated their role in the induction of IpaD-mediated B cell apoptosis. On the one hand, by timely modulation of the expression of pro- and anti-apoptotic proteins, such as Bad/Bax and Bcl-2/Bcl-xl, respectively, and induction of a loss of MMP, bacterial co-signals sensitize B cells, rendering them prone to die. On the other hand, they lead to the up-regulation of TLR2 transcript expression, thus promoting the TLR2–IpaD interaction. The loss of MMP has previously been demonstrated for the induction of necrotic and apoptotic death of epithelial cells upon *Shigella* infection (Koterski et al., 2005; Carneiro et al., 2009; Lembo-Fazio et al., 2011). Additionally, B cell death induced by *F. tularensis* and *H. pylori* was also described to be apoptotic and accompanied by release of apoptosis-inducing factor (AIF) from mitochondria (Singh et al., 2006; Zivna et al., 2010).

Altogether, these findings lead us to propose a working model for *Shigella* interaction with B lymphocytes: *S. flexneri* is able to invade B cells and proliferate intracellularly, resulting in cell death. Additionally, B cell death occurs independently from invasion or translocation of virulence effectors. *Shigella*-induced B cell apoptosis of noninvaded cells results from the integration of two different types of signals: (1) bacterial co-signals sensitize B cells to apoptosis and enhance the basal level of TLR2 gene expression; (2) by the resulting increased interaction with TLR2, IpaD tips the balance of signaling pathways toward a deadly fate. Whether or not such a strategy is used by other bacterial pathogens and takes place in other host cell types deserves further investigation.

In conclusion, our findings add to the diversity of mechanisms used by *Shigella* to manipulate the adaptive immune response. Indeed, the work presented here reveals a direct targeting of B cells by *Shigella*, a finding which could explain why this disease does not induce antibody-mediated lasting immunity. It could also explain the difficulties encountered in *Shigella* vaccine development, especially for the live, attenuated vaccine candidates whose design did not take into account the immunosuppressive capacities of *Shigella* we recently highlighted (Konradt et al., 2011; Salgado-Pabón et al., 2013). This study highlights that manipulation of B lymphocytes resulting from direct interactions with pathogens must be considered when deciphering the efficiency of protective B cell responses to infection.

MATERIALS AND METHODS

Bacterial strains. The *S. flexneri* strains used in this study are listed in Table S2. Bacteria were grown at 37°C on trypticase soy agar (TSA; BD) plates containing 0.01% Congo red (Serva). Single colonies were picked for overnight culture at 37°C in trypticase soy broth, followed by a subculture inoculated at a 1/50 dilution. Bacteria were prepared for infections in late exponential growth phase and inoculi were calculated from the optical density of the culture at 600 nm. The *S. flexneri* strains were centrifuged at 4,000 *g* for 10 min and resuspended in culture medium to a defined inoculum for infection. To generate bacterial lysates, bacteria were incubated with 50 µg/ml gentamicin for 45 min at 37°C, sonicated, or heat killed for 45 min at 65°C. Inoculi were controlled by plating dilutions of bacterial suspensions on TSA plates. Bacterial PAMPs used in the experiments included Ultrapure *E. Coli* LPS (25 µg/ml; InvivoGen), PGN-ECndss Ultrapure (25 µg/ml; InvivoGen), and ODN 2006 CpG (10 µg/ml; InvivoGen).

Biopsies of *Shigella*-infected patients. Adult patients clinically suspected of having dysentery within 3–4 d of onset of disease were initially enrolled at the International Center for Diarrheal Diseases Research, Bangladesh (ICDDR,B). The collection of biopsies from patients for studying immunological/immunopathological responses was approved by the Ethical Review Committee of ICDDR,B. Patients were diagnosed for shigellosis after overnight stool culture on McKonkey and *Shigella Salmonella* (SS) agar plates. Confirmation of diagnosis was achieved by testing for *Shigella* spp. by agglutination to specific antisera and further biochemical tests. Proctoscopy (long-speculum Anoscope; Welch Allyn series 31610) was performed to obtain rectal biopsy specimens from each patient within 48 h of admission at ∼10–12 cm from the anus into the rectum. Formalin-fixed, paraffin-embedded tissues were sectioned at 3-µm thickness with a microtome (RM 2055; Leica) and stored at room temperature until analysis. Biopsies from 12 patients were analyzed by immunofluorescence. Image representation was focused on patients presenting severe shigellosis ($n = 4$) in whose biopsies we could identify a lymphoid follicle ($n = 2$).

Ex vivo infections of human colonic tissues. Tissue specimens were obtained from patients who underwent surgery for colonic adenocarcinoma, according to the guidelines of the French Ethics Committee for Research on Human Tissues. Specimens were taken at a distance from the tumor in macroscopically and histologically normal areas and immediately processed in the pathology department. According to the guidelines of the French Ethics Committee for Research on Human Tissues, these specimens were considered to be residual tissue, and not relevant to pathological diagnosis.

Ex vivo infections were performed as described in Coron et al. (2009). In brief, the serosa and muscle layers were dissected under a stereomicroscope and excess mucus removed by carefully dabbing the tissue with a paper towel. The specimens were cut into ∼5-cm^2 segments and pinned flat, with the submucosa facing down, onto a 4% agarose layer in tissue culture Petri dishes containing DMEM/F12 culture medium (Invitrogen) supplemented with 10% FBS, glutamine, and 2.1 g/liter $NaHCO_3$ (Sigma-Aldrich). *S. flexneri* WT bacteria and the T3SA$^-$ mutant were added at ∼2×10^8 bacteria per cm^2 of tissue. Bacteria were allowed to settle for 15 min at room temperature before incubation of infected and uninfected control tissue at 37°C, 5% CO_2 for 6 h on a slowly rocking tray. Tissue was fixed by overnight incubation with 4% PFA (Euromedex) and 0.1 M Hepes (Gibco) in PBS. Tissue pieces were embedded in paraffin and sectioned at 9 µm with a microtome (RM2145; Leica) for histological analyses. For whole-mount staining, tissues were fixed on a 40 × 11–mm tissue culture dish (TPP) with Histoacryl tissue glue (Braun). To obtain 150-µm-thick sections, the tissue was embedded in low-melting agarose according to Snippert et al. (2011) and cut with a vibratome (VT1000E; Leica).

Mouse in vivo footpad infections. Pathogen-free, female C57BL/6 mice (6–8 wk of age) were purchased from Janvier and kept at the Institut Pasteur animal facilities. All procedures involving animals were approved by the Safety Committee of the Institut Pasteur in accordance with French and European guidelines. Mice were infected subcutaneously in the footpad with 1–3 × 10^8 WT or T3SA$^-$ bacteria in 50 µl PBS, and sacrificed at 24 and 48 h p.i. for popliteal LN extraction as previously described (Salgado-Pabón et al., 2013).

In vitro B cell infections. The CL-01 cell line (Cerutti et al., 1998; provided by A. Cerutti, IMIM, Barcelona, Spain) was maintained at a density between 2 × 10^4 and 2 × 10^5 cells per ml in RPMI 1640 (Invitrogen)

supplemented with 10% FBS (Biowest) at 37°C, 5% CO_2. B cells were seeded in round-bottomed 96-well plates (TPP) at a concentration of 1–3 × 10^5 cells in 100 µl per well. Bacteria were added in cell culture medium to a multiplicity of infection (MOI) of 50 in 50 µl per well, and centrifuged onto the cells for 5 min at 300 *g*. Infected cells were incubated at 37°C, 5% CO_2. Gentamicin was added at 30 min p.i. to a final concentration of 50 µg/ml (50 µl/well at 200 µg/ml). Intracellular bacteria were quantified upon cell lysis with 0.5% sodium desoxycholate followed by plating on TSA plates.

Expression and purification of recombinant IpaD. Expression of recombinant, C-terminally His-tagged IpaD and MxiH (the latter lacking the last five C-terminal residues) was performed in *E. coli* BL21. Bacteria were cultured in LB media for 3 h at 37°C, harvested by centrifugation for 20 min at 15,000 *g*, and resuspended in PBS, pH 8, containing 100 mg/ml lysozyme, 1 mM $MgCl_2$, and 0.1% Triton X-100. The resulting suspension was incubated for 15 min at 4°C before addition of 10 U Benzonase and sonication until the suspension lost viscosity. Bacterial fragments were removed by centrifugation for 20 min at 15,000 *g* and recombinant His-tagged proteins localized in the supernatant were purified by nickel chelation chromatography (AKTA system, IMAC-Nickel chelating, Hi-Trap FF; GE Healthcare). Proteins were washed and eluted using buffers containing imidazole. Fractions containing the protein were pooled and dialyzed against PBS. Purity of the preparation was checked by gel electrophoresis and Coomassie staining (one 37.5 kD band detected for 3 µg protein) and LAL endotoxin levels were determined to be <500 U/mg (Endosafe; Charles River). For fluorescent detection, purified His-tagged IpaD and MxiH were labeled with Alexa Fluor 488 Microscale Protein Labeling kit (Invitrogen) according to the manufacturer's instructions.

If not otherwise indicated, IpaD and MxiH were added at 5 µg/well (25 µg/ml) in parallel to the infection. For blocking experiments, cells were preincubated with T3SA$^-$ bacteria for 22 h and subsequently incubated with 10 µg/ml functional grade purified α-TLR2 (eBioscience) or α-TLR1 (eBioscience) before addition of 10 µg/ml IpaD for 6 h. The same concentration and set-up was used for testing TLR2-agonists FSL-1 (InvivoGen) and Pam3CSK4 (InvivoGen).

Flow cytometry. Quantification of cell number and assessment of cell death were achieved by addition of both a defined number of fluorescently labeled CaliBRITE beads (BD) and propidium iodide (PI; 1:3,000; Sigma-Aldrich) to cell suspensions. For assessment of apoptosis, cells were co-stained with APC Annexin V (BD) according to manufacturer's instructions before addition of beads and PI. Cells obtained from LNs of *Shigella*-infected mice were co-stained with α-CD19 FITC (1:100; eBioscience) and α-CD4 PE (1:100; eBioscience). Loss of MMP was assessed by use of the JC-1 probe (mitochondrial staining kit; Sigma-Aldrich) according to manufacturer's instructions. Samples were acquired on a FACSCalibur or Canto II (BD) and analyzed with FlowJo software.

Immunofluorescence staining. Primary antibodies used for human intestinal tissues included α-CD20cy and α–plasma cell (1:75; Dako) for B cells, α-CD3 (1:75; Dako) for T cells, and rabbit polyclonal antibodies specific for *S. flexneri* 5a and IpaD (collection of the laboratory). Secondary antibodies coupled to Cy3, Cy5, or Alexa Fluor 488 were purchased from Jackson ImmunoResearch Laboratories, Inc. TUNEL staining was performed with the In situ cell death detection kit according to the manufacturer's instructions (BD). As opposed to classical histological staining, whole-mount staining was achieved by increasing incubation times considerably. Vibratome sections were stained as previously described (Snippert et al., 2011). B cells incubated in vitro with fluorescent IpaD and MxiH were co-stained with 1 µg/ml Cholera Toxin B-Subunit (CTxB) coupled to Alexa Fluor 555 (Molecular Probes) at 4°C before and with 2 µg/ml DAPI (Invitrogen) after fixation with 4% PFA. Coverslips were mounted using ProLong-mounting medium (Invitrogen) for short-term preservation, whereas whole-mount tissue and vibratome sections were imaged shortly after the staining procedure. Fluorescence images were acquired either by inverted wide-field (Observer Z1; Carl Zeiss) or confocal microscopy (SP5, Leica; LSM710, Carl Zeiss) and analyzed using Fiji (ImageJ, National Institutes of Health) and Imaris (Bitplane) software.

Adjustments of settings, brightness, and contrast were only applied for representative images. Acquisition of images used for quantification was performed on the same day with the same acquisition settings and no image adjustments. AF488 mean fluorescence intensity (MFI) was quantified within 15-µm spheres centered on DAPI fluorescence using Imaris software. The relative values of conditions were only compared within each experiment, and data are presented for one representative experiment out of a minimum of two independent experiments.

Quantification of IpaD internalization into CL-01 cells. The following protocol was adapted from Malhotra et al. (2009). In brief, CL-01 cells were incubated with fluorescent IpaD-AF488 as described above for 1 h at 4°C. Subsequently, cells were washed and incubated at 37°C for 30 min or 1 h. IpaD bound to the cell surface was analyzed by flow cytometry, using an anti-IpaD polyclonal serum (1:100) and a secondary antibody coupled to Alexa Fluor 647 (1:500; Life Technologies). The AF488 signal was used as control to monitor that the total amount of protein associated to the cell does not decrease during the time course of the experiment. The percentage of surface-bound IpaD was calculated as percentage of AF647 fluorescence intensity after incubation at 37°C versus the intensity after incubation at 4°C (time point 0). Data are presented as the percentage of surface bound IpaD at time point 0 minus the percentage of surface bound IpaD at the respective time points, thus corresponding to the percentage of IpaD that has been internalized at 37°C.

SDS-PAGE and immunoblotting. Cells were infected as described above and lysed in 100 µl Laemmli buffer (Bio-Rad Laboratories) per 0.5–1.5 × 10^6 cells. Protein quantification was achieved using the EZQ Protein quantitation kit (Molecular Probes). Between 25 and 125 µg of proteins was resolved on mini-protean TGX gels (Bio-Rad Laboratories) in Tris/glycine/SDS running buffer (Bio-Rad Laboratories) and transferred to PVDF membranes using the iBlot system (Invitrogen). Membranes were blocked for 2 h in 5% milk in TBS containing 0.01% Tween 20 (TBST; Sigma-Aldrich) and incubated with primary antibodies overnight at 4°C. Primary antibodies and concentrations used are given in Table S4. Detection was achieved with α-rabbit (Jackson ImmunoResearch Laboratories, Inc.) or α-mouse (GE Healthcare) HRP-conjugated secondary antibodies and SuperSignal West chemiluminescent substrates (Thermo Fisher Scientific). Pixel intensities were quantified with Fiji imaging software (ImageJ) and presented as fold change over uninfected after normalization to actin protein amounts. The Human Apoptosis Array kit (R&D Systems) was used according to manufacturer's instructions with 2.5 × 10^6 cells infected in 15-ml round-bottomed falcon tubes for 5 h.

Gene expression quantification. 1 × 10^6 cells were collected as cell pellet, either uninfected or after infection as described above. RNA was extracted and cDNA generated using the RNeasy Mini (QIAGEN) and Superscript III Reverse transcription (Life Technologies) kits, respectively, according to manufacturer's instructions. FastStart SYBR Green Master Mix (Roche) was used according to the manufacturer's instructions and thermo cycling was fixed to 95°C for 5 min, followed by 40 cycles of 95°C for 10 s, 60°C for 45 s, and 72°C for 45 s. Forward and reverse primers were used at a final concentration of 1 µM and are given in Table S3. Relative expression was calculated based on β-ACT normalization after experimental comparison with cyclophilin A (PPIA). All reactions were run in duplicate. Primers were validated with the use of FACS-sorted (>99% pure) human primary cells (Etablissement Français du Sang [EFS]) known to express the respective TLR transcript. Postreaction melt curve analysis was conducted to ensure that peak melting temperature remained within ±0.5°C of the positive control and transcript levels were expressed according to the following formula: Relative Expression = $1{,}000*2^{-(\Delta CT)}$.

RNA interference. Transfection conditions for the CL-01 cell line were established using Control siRNA (FITC Conjugate)-A (Santa Cruz Biotechnology, Inc.) and the Cell Line Nucleofector kit V on the Amaxa system (Lonza), and set to 1.8 µM siRNA for 3 × 10^6 cells in 100 µl, program A-023.

Cells were transfected with SMARTpool ON-TARGETplus TLR2 (Thermo Fisher Scientific; L-005120-01-0005), TLR10 (L-008087-00-0005), TLR1 (L-008086-00-0005), or TLR6 (L-005156-00-0005) siRNA or the ON-TARGETplus Non-targeting Pool (Thermo Fisher Scientific; D-001810-10-05). Efficiency of interference was assessed by gene expression quantification 24 h after transfection and mRNA levels were reduced to 52, 83, 34, and 31% for TLR1, TLR2, TLR6, and TLR10, respectively. Infections of transfected cells were performed at this time point as described above.

TLR2 cell-based reporter assay. To assess the signaling activity of IpaD via TLR2, we used the cell-based reporter assay described in Burger-Kentischer et al. (2010). The Assay was performed with the two reporter cell lines NIH3T3 PRR SEAP TLR2-1 and TLR2-6, and the control cell line NIH3T3 SEAP. Cells were seeded in a 96-well plate at a density of 0.3×10^5 cells/well in a final volume of 100 µl culture medium (DMEM supplemented with 10% FCS, 50 U/ml penicillin, 0.05 mg/ml streptomycin, and 2 mmol/liter L-glutamine). After a cultivation period of 25 h, media were replaced with the respective volume of fresh medium (DMEM, 0.5% FCS), including test samples (different concentrations of IpaD) and controls. Controls included sample buffer PBS, pH 7.0 (negative control), TNF 500 ng/ml (positive control, control cell line without TLR), Pam3CysSK4 1 µg/ml (positive control, TLR2-1 reporter cell line), and FSL-1 1 µg/ml (positive control, TLR2-6 reporter cell line). The spiked control represents the test sample (1 µg/ml IpaD) spiked with the respective positive control. Induction was performed for 18 h at 37°C and 5% CO_2 and SEAP was detected in the supernatant by use of the substrate (pNPP; *p*-nitrophenyl phosphate). Plates were read using an UV-VIS reader at 405 nm and the software SoftMaxPro (version 5.01; Molecular Devices) for data recording.

Data presentation and statistical analysis. Prism 5.0 (GraphPad Software) was used for graphs, and statistical analyses and figures were created using Inkscape software. The Mann Whitney unpaired Student's *t* test was used to compare two groups, and one-way and two-way ANOVA with Bonferroni post-test for comparison of multiple groups and conditions.

Online supplemental material. Video 1 presents an animation of confocal imaging of 150-µm-thick tissue sections and shows that *S. flexneri* is found intracellular in B lymphocytes within ILFs. Table S1 shows the regulation of pro- and anti-apoptotic proteins after infection as assessed by a protein-based Apoptosis Array. Tables S2, S3, and S4 present lists of *S. flexneri* strains used in the experiments, primers used for gene expression quantification, and antibodies used for immunoblotting, respectively. Online supplemental material is available at http://www.jem.org/cgi/content/full/jem.20130914/DC1.

We thank the Institut Pasteur Imagopole (PFID) for their contribution to imaging studies, Andrea Cerrutti for kindly providing us with the CL-01 B cell line, and Philippe Aubert, Angela Mattes, and Françoise Thouron for technical help and kind assistance. We are grateful to several people who have contributed to this work with helpful discussions, advice, and critical reading of the manuscript, namely Paulo Vieira, Gérard Eberl, François Huetz, Jean-Claude Weill, Menno van Zelm, Bana Jabri, Geneviève Renauld, Paul Erlich, Daniel Scott, Nathalie Sauvonnet, Christoph Konradt, Elisabetta Frigimelica, Giulia Nigro, François-Xavier Campbell-Valois, and the whole PMM unit.

K. Nothelfer was funded by the Pasteur-Paris University International PhD Program, the Pasteur Weizmann Foundation, and the Transversal Research Program (project no. 415). E.T. Arena is a Pasteur Foundation fellow and L. Pinaud is a fellow from the University Paris Diderot. I. Belotserkovsky has received funding from the French Ministry of Foreign Affairs and the Transversal Research Program (project no. 415). P.J. Sansonetti is supported by the European Research Council (ERC; project Homeopith); he is a Howard Hughes Medical Institute Foreign Scholar. This study has received funding from the French Government's Investissement d'Avenir program, Laboratoire d'Excellence "Integrative Biology of Emerging Infectious Diseases" (grant no. ANR-10-LABEX-62-IBEID).

The authors declare no competing financial interests.

Submitted: 2 May 2013
Accepted: 15 April 2014

REFERENCES

Acosta Rodriguez, E.V., E.I. Zuniga, C.L. Montes, M.C. Merino, D.A. Bermejo, M.C. Amezcua Vesely, C.C. Motran, and A. Gruppi. 2007. *Trypanosoma cruzi* infection beats the B-cell compartment favouring parasite establishment: can we strike first? *Scand. J. Immunol.* 66:137–142. http://dx.doi.org/10.1111/j.1365-3083.2007.01968.x

Ahmed, F., J.D. Clemens, M.R. Rao, D.A. Sack, M.R. Khan, and E. Haque. 1992. Community-based evaluation of the effect of breast-feeding on the risk of microbiologically confirmed or clinically presumptive shigellosis in Bangladeshi children. *Pediatrics*. 90:406–411.

Aliprantis, A.O., R.B. Yang, M.R. Mark, S. Suggett, B. Devaux, J.D. Radolf, G.R. Klimpel, P. Godowski, and A. Zychlinsky. 1999. Cell activation and apoptosis by bacterial lipoproteins through toll-like receptor-2. *Science*. 285:736–739. http://dx.doi.org/10.1126/science.285.5428.736

Aliprantis, A.O., R.B. Yang, D.S. Weiss, P. Godowski, and A. Zychlinsky. 2000. The apoptotic signaling pathway activated by Toll-like receptor-2. *EMBO J.* 19:3325–3336. http://dx.doi.org/10.1093/emboj/19.13.3325

Bhunia, A.K., and X. Feng. 1999. Examination of cytopathic effect and apoptosis in *Listeria monocytogenes*-infected hybridoma B-lymphocyte (Ped-2E9) line in vitro. *J. Microbiol. Biotechnol.* 9:398–403.

Blocker, A., P. Gounon, E. Larquet, K. Niebuhr, V. Cabiaux, C. Parsot, and P. Sansonetti. 1999. The tripartite type III secreton of *Shigella flexneri* inserts IpaB and IpaC into host membranes. *J. Cell Biol.* 147:683–693. http://dx.doi.org/10.1083/jcb.147.3.683

Burger-Kentischer, A., I.S. Abele, D. Finkelmeier, K.-H. Wiesmüller, and S. Rupp. 2010. A new cell-based innate immune receptor assay for the examination of receptor activity, ligand specificity, signalling pathways and the detection of pyrogens. *J. Immunol. Methods*. 358:93–103. http://dx.doi.org/10.1016/j.jim.2010.03.020

Carneiro, L.A.M., L.H. Travassos, F. Soares, I. Tattoli, J.G. Magalhaes, M.T. Bozza, M.C. Plotkowski, P.J. Sansonetti, J.D. Molkentin, D.J. Philpott, and S.E. Girardin. 2009. *Shigella* induces mitochondrial dysfunction and cell death in nonmyleoid cells. *Cell Host Microbe*. 5:123–136. http://dx.doi.org/10.1016/j.chom.2008.12.011

Castro-Eguiluz, D., R. Pelayo, V. Rosales-Garcia, R. Rosales-Reyes, C. Alpuche-Aranda, and V. Ortiz-Navarrete. 2009. B cell precursors are targets for *Salmonella* infection. *Microb. Pathog.* 47:52–56. http://dx.doi.org/10.1016/j.micpath.2009.04.005

Cerutti, A., H. Zan, A. Schaffer, L. Bergsagel, N. Harindranath, E.E. Max, and P. Casali. 1998. CD40 ligand and appropriate cytokines induce switching to IgG, IgA, and IgE and coordinated germinal center and plasmacytoid phenotypic differentiation in a human monoclonal IgM^+IgD^+ B cell line. *J. Immunol.* 160:2145–2157.

Clemens, J.D., B. Stanton, B. Stoll, N.S. Shahid, H. Banu, and A.K. Chowdhury. 1986. Breast feeding as a determinant of severity in shigellosis. Evidence for protection throughout the first three years of life in Bangladeshi children. *Am. J. Epidemiol.* 123:710–720.

Coron, E., M. Flamant, P. Aubert, T. Wedel, T. Pedron, E. Letessier, J.P. Galmiche, P.J. Sansonetti, and M. Neunlist. 2009. Characterisation of early mucosal and neuronal lesions following *Shigella flexneri* infection in human colon. *PLoS ONE*. 4:e4713. http://dx.doi.org/10.1371/journal.pone.0004713

Crampton, S.P., E. Voynova, and S. Bolland. 2010. Innate pathways to B-cell activation and tolerance. *Ann. N.Y. Acad. Sci.* 1183:58–68. http://dx.doi.org/10.1111/j.1749-6632.2009.05123.x

Edgeworth, J.D., J. Spencer, A. Phalipon, G.E. Griffin, and P.J. Sansonetti. 2002. Cytotoxicity and interleukin-1β processing following *Shigella flexneri* infection of human monocyte-derived dendritic cells. *Eur. J. Immunol.* 32:1464–1471. http://dx.doi.org/10.1002/1521-4141(200205)32:5<1464::AID-IMMU1464>3.0.CO;2-G

Epler, C.R., N.E. Dickenson, E. Bullitt, and W.L. Picking. 2012. Ultrastructural analysis of IpaD at the tip of the nascent MxiH type III secretion apparatus of *Shigella flexneri*. *J. Mol. Biol.* 420:29–39. http://dx.doi.org/10.1016/j.jmb.2012.03.025

Espina, M., A.J. Olive, R. Kenjale, D.S. Moore, S.F. Ausar, R.W. Kaminski, E.V. Oaks, C.R. Middaugh, W.D. Picking, and W.L. Picking. 2006. IpaD localizes to the tip of the type III secretion system needle of *Shigella flexneri*. *Infect. Immun.* 74:4391–4400. http://dx.doi.org/10.1128/IAI.00440-06

Espina, M., S.F. Ausar, C.R. Middaugh, M.A. Baxter, W.D. Picking, and W.L. Picking. 2007. Conformational stability and differential structural analysis of LcrV, PcrV, BipD, and SipD from type III secretion systems. *Protein Sci.* 16:704–714. http://dx.doi.org/10.1110/ps.062645007

Finlay, B.B., and G. McFadden. 2006. Anti-immunology: evasion of the host immune system by bacterial and viral pathogens. *Cell.* 124:767–782. http://dx.doi.org/10.1016/j.cell.2006.01.034

Flashner, Y., M. Fisher, A. Tidhar, A. Mechaly, D. Gur, G. Halperin, E. Zahavy, E. Mamroud, and S. Cohen. 2010. The search for early markers of plague: evidence for accumulation of soluble *Yersinia pestis* LcrV in bubonic and pneumonic mouse models of disease. *FEMS Immunol. Med. Microbiol.* 59:197–206.

Goenka, R., P.D. Guirnalda, S.J. Black, and C.L. Baldwin. 2012. B Lymphocytes provide an infection niche for intracellular bacterium *Brucella abortus*. *J. Infect. Dis.* 206:91–98. http://dx.doi.org/10.1093/infdis/jis310

Graves, J.D., A. Craxton, and E.A. Clark. 2004. Modulation and function of caspase pathways in B lymphocytes. *Immunol. Rev.* 197:129–146. http://dx.doi.org/10.1111/j.0105-2896.2004.0110.x

Hornef, M.W., M.J. Wick, M. Rhen, and S. Normark. 2002. Bacterial strategies for overcoming host innate and adaptive immune responses. *Nat. Immunol.* 3:1033–1040. http://dx.doi.org/10.1038/ni1102-1033

Hornung, V., S. Rothenfusser, S. Britsch, A. Krug, B. Jahrsdörfer, T. Giese, S. Endres, and G. Hartmann. 2002. Quantitative expression of toll-like receptor 1-10 mRNA in cellular subsets of human peripheral blood mononuclear cells and sensitivity to CpG oligodeoxynucleotides. *J. Immunol.* 168:4531–4537. http://dx.doi.org/10.4049/jimmunol.168.9.4531

Islam, M.M., A.K. Azad, P.K. Bardhan, R. Raqib, and D. Islam. 1994. Pathology of shigellosis and its complications. *Histopathology.* 24:65–71. http://dx.doi.org/10.1111/j.1365-2559.1994.tb01272.x

Jendholm, J., M. Mörgelin, M.L.A. Perez Vidakovics, M. Carlsson, H. Leffler, L.O. Cardell, and K. Riesbeck. 2009. Superantigen- and TLR-dependent activation of tonsillar B cells after receptor-mediated endocytosis. *J. Immunol.* 182:4713–4720. http://dx.doi.org/10.4049/jimmunol.0803032

Johnson, S., P. Roversi, M. Espina, A. Olive, J.E. Deane, S. Birket, T. Field, W.D. Picking, A.J. Blocker, E.E. Galyov, et al. 2007. Self-chaperoning of the type III secretion system needle tip proteins IpaD and BipD. *J. Biol. Chem.* 282:4035–4044. http://dx.doi.org/10.1074/jbc.M607945200

Kim, D.W., H. Chu, D.H. Joo, M.S. Jang, J.H. Choi, S.-M. Park, Y.-J. Choi, S.H. Han, and C.-H. Yun. 2008. OspF directly attenuates the activity of extracellular signal-regulated kinase during invasion by *Shigella flexneri* in human dendritic cells. *Mol. Immunol.* 45:3295–3301. http://dx.doi.org/10.1016/j.molimm.2008.02.013

Konradt, C., E. Frigimelica, K. Nothelfer, A. Puhar, W. Salgado-Pabon, V. di Bartolo, D. Scott-Algara, C.D. Rodrigues, P.J. Sansonetti, and A. Phalipon. 2011. The *Shigella flexneri* type three secretion system effector IpgD inhibits T cell migration by manipulating host phosphoinositide metabolism. *Cell Host Microbe.* 9:263–272. http://dx.doi.org/10.1016/j.chom.2011.03.010

Koterski, J.F., M. Nahvi, M.M. Venkatesan, and B. Haimovich. 2005. Virulent *Shigella flexneri* causes damage to mitochondria and triggers necrosis in infected human monocyte-derived macrophages. *Infect. Immun.* 73:504–513. http://dx.doi.org/10.1128/IAI.73.1.504-513.2005

Krocova, Z., A. Härtlova, D. Souckova, L. Zivna, M. Kroca, E. Rudolf, A. Macela, and J. Stulik. 2008. Interaction of B cells with intracellular pathogen *Francisella tularensis*. *Microb. Pathog.* 45:79–85. http://dx.doi.org/10.1016/j.micpath.2008.01.010

Lampropoulou, V., E. Calderon-Gomez, T. Roch, P. Neves, P. Shen, U. Stervbo, P. Boudinot, S.M. Anderton, and S. Fillatreau. 2010. Suppressive functions of activated B cells in autoimmune diseases reveal the dual roles of Toll-like receptors in immunity. *Immunol. Rev.* 233:146–161. http://dx.doi.org/10.1111/j.0105-2896.2009.00855.x

Lembo-Fazio, L., G. Nigro, G. Noël, G. Rossi, F. Chiara, K. Tsilingiri, M. Rescigno, A. Rasola, and M.L. Bernardini. 2011. Gadd45α activity is the principal effector of *Shigella* mitochondria-dependent epithelial cell death in vitro and ex vivo. *Cell Death Dis.* 2:e122. http://dx.doi.org/10.1038/cddis.2011.4

Lunelli, M., R. Hurwitz, J. Lambers, and M. Kolbe. 2011. Crystal structure of PrgI-SipD: insight into a secretion competent state of the type three secretion system needle tip and its interaction with host ligands. *PLoS Pathog.* 7:e1002163. http://dx.doi.org/10.1371/journal.ppat.1002163

Machida, K., Y. Kondo, J.Y. Huang, Y.C. Chen, K.T.H. Cheng, Z. Keck, S. Foung, J. Dubuisson, V.M.H. Sung, and M.M.C. Lai. 2008. Hepatitis C virus (HCV)-induced immunoglobulin hypermutation reduces the affinity and neutralizing activities of antibodies against HCV envelope protein. *J. Virol.* 82:6711–6720. http://dx.doi.org/10.1128/JVI.02582-07

Malhotra, S., S. Kovats, W. Zhang, and K.M. Coggeshall. 2009. B cell antigen receptor endocytosis and antigen presentation to T cells require Vav and dynamin. *J. Biol. Chem.* 284:24088–24097. http://dx.doi.org/10.1074/jbc.M109.014209

Månsson, A., M. Adner, U. Höckerfelt, and L.-O. Cardell. 2006. A distinct Toll-like receptor repertoire in human tonsillar B cells, directly activated by PamCSK, R-837 and CpG-2006 stimulation. *Immunology.* 118:539–548.

Ménard, R., P.J. Sansonetti, and C. Parsot. 1993. Nonpolar mutagenesis of the ipa genes defines IpaB, IpaC, and IpaD as effectors of *Shigella flexneri* entry into epithelial cells. *J. Bacteriol.* 175:5899–5906.

Ménard, R., P. Sansonetti, and C. Parsot. 1994. The secretion of the *Shigella flexneri* Ipa invasins is activated by epithelial cells and controlled by IpaB and IpaD. *EMBO J.* 13:5293–5302.

Menon, A., M.L. Shroyer, J.L. Wampler, C.B. Chawan, and A.K. Bhunia. 2003. In vitro study of *Listeria monocytogenes* infection to murine primary and human transformed B cells. *Comp. Immunol. Microbiol. Infect. Dis.* 26:157–174. http://dx.doi.org/10.1016/S0147-9571(02)00039-5

Miller, C.L., J.H. Lee, E. Kieff, and R. Longnecker. 1994. An integral membrane protein (LMP2) blocks reactivation of Epstein-Barr virus from latency following surface immunoglobulin crosslinking. *Proc. Natl. Acad. Sci. USA.* 91:772–776. http://dx.doi.org/10.1073/pnas.91.2.772

Minoprio, P., O. Burlen, P. Pereira, B. Guilbert, L. Andrade, M. Hontebeyrie-Joskowicz, and A. Coutinho. 1988. Most B cells in acute *Trypanosoma cruzi* infection lack parasite specificity. *Scand. J. Immunol.* 28:553–561. http://dx.doi.org/10.1111/j.1365-3083.1988.tb01487.x

Moraes, T.F., T. Spreter, and N.C. Strynadka. 2008. Piecing together the type III injectisome of bacterial pathogens. *Curr. Opin. Struct. Biol.* 18:258–266. http://dx.doi.org/10.1016/j.sbi.2007.12.011

Oberhelman, R.A., D.J. Kopecko, E. Salazar-Lindo, E. Gotuzzo, J.M. Buysse, M.M. Venkatesan, A. Yi, C. Fernandez-Prada, M. Guzman, R. León-Barúa, et al. 1991. Prospective study of systemic and mucosal immune responses in dysenteric patients to specific *Shigella* invasion plasmid antigens and lipopolysaccharides. *Infect. Immun.* 59:2341–2350.

Pantelic, M., Y.J. Kim, S. Bolland, I. Chen, J. Shively, and T. Chen. 2005. *Neisseria gonorrhoeae* kills carcinoembryonic antigen-related cellular adhesion molecule 1 (CD66a)-expressing human B cells and inhibits antibody production. *Infect. Immun.* 73:4171–4179. http://dx.doi.org/10.1128/IAI.73.7.4171-4179.2005

Parsot, C. 2009. *Shigella* type III secretion effectors: how, where, when, for what purposes? *Curr. Opin. Microbiol.* 12:110–116. http://dx.doi.org/10.1016/j.mib.2008.12.002

Phalipon, A., and P.J. Sansonetti. 2007. *Shigella*'s ways of manipulating the host intestinal innate and adaptive immune system: a tool box for survival? *Immunol. Cell Biol.* 85:119–129. http://dx.doi.org/10.1038/sj.icb7100025

Pone, E.J., H. Zan, J. Zhang, A. Al-Qahtani, Z. Xu, and P. Casali. 2010. Toll-like receptors and B-cell receptors synergize to induce immunoglobulin class-switch DNA recombination: relevance to microbial antibody responses. *Crit. Rev. Immunol.* 30:1–29. http://dx.doi.org/10.1615/CritRevImmunol.v30.i1.10

Raqib, R., A.A. Lindberg, L. Björk, P.K. Bardhan, B. Wretlind, U. Andersson, and J. Andersson. 1995. Down-regulation of gamma interferon, tumor necrosis factor type I, interleukin 1 (IL-1) type I, IL-3, IL-4, and transforming growth factor beta type I receptors at the local site during the acute phase of Shigella infection. *Infect. Immun.* 63:3079–3087.

Raqib, R., S.M. Mia, F. Qadri, T.I. Alam, N.H. Alam, A.K. Chowdhury, M.M. Mathan, and J. Andersson. 2000. Innate immune responses in children and adults with Shigellosis. *Infect. Immun.* 68:3620–3629. http://dx.doi.org/10.1128/IAI.68.6.3620-3629.2000

Raqib, R., F. Qadri, P. SarkEr, S.M. Mia, P.J. Sansonnetti, M.J. Albert, and J. Andersson. 2002. Delayed and reduced adaptive humoral immune responses in children with shigellosis compared with in adults.

Scand. J. Immunol. 55:414–423. http://dx.doi.org/10.1046/j.1365-3083.2002.01079.x

Rawlings, D.J., M.A. Schwartz, S.W. Jackson, and A. Meyer-Bahlburg. 2012. Integration of B cell responses through Toll-like receptors and antigen receptors. *Nat. Rev. Immunol.* 12:282–294. http://dx.doi.org/10.1038/nri3190

Ruprecht, C.R., and A. Lanzavecchia. 2006. Toll-like receptor stimulation as a third signal required for activation of human naive B cells. *Eur. J. Immunol.* 36:810–816. http://dx.doi.org/10.1002/eji.200535744

Salgado-Pabón, W., S. Celli, E.T. Arena, K. Nothelfer, P. Roux, G. Sellge, E. Frigimelica, P. Bousso, P.J. Sansonetti, and A. Phalipon. 2013. *Shigella* impairs T lymphocyte dynamics in vivo. *Proc. Natl. Acad. Sci. USA.* 110: 4458–4463. http://dx.doi.org/10.1073/pnas.1300981110

Sani, M., A. Botteaux, C. Parsot, P. Sansonetti, E.J. Boekema, and A. Allaoui. 2007. IpaD is localized at the tip of the *Shigella flexneri* type III secretion apparatus. *Biochim. Biophys. Acta.* 1770:307–311. http://dx.doi.org/10.1016/j.bbagen.2006.10.007

Sansonetti, P.J., and J.P. Di Santo. 2007. Debugging how bacteria manipulate the immune response. *Immunity.* 26:149–161. http://dx.doi.org/10.1016/j.immuni.2007.02.004

Sellge, G., J.G. Magalhaes, C. Konradt, J.H. Fritz, W. Salgado-Pabon, G. Eberl, A. Bandeira, J.P. Di Santo, P.J. Sansonetti, and A. Phalipon. 2010. Th17 cells are the dominant T cell subtype primed by *Shigella flexneri* mediating protective immunity. *J. Immunol.* 184:2076–2085. http://dx.doi.org/10.4049/jimmunol.0900978

Sen, R. 2006. Control of B lymphocyte apoptosis by the transcription factor NF-κB. *Immunity.* 25:871–883. http://dx.doi.org/10.1016/j.immuni.2006.12.003

Sing, A., D. Rost, N. Tvardovskaia, A. Roggenkamp, A. Wiedemann, C.J. Kirschning, M. Aepfelbacher, and J. Heesemann. 2002. Yersinia V–antigen exploits toll-like receptor 2 and CD14 for interleukin 10–mediated immunosuppression. *J. Exp. Med.* 196:1017–1024. http://dx.doi.org/10.1084/jem.20020908

Singh, M., K.N. Prasad, A. Saxena, and S.K. Yachha. 2006. *Helicobacter pylori* induces apoptosis of T- and B-cell lines and translocates mitochondrial apoptosis-inducing factor to nucleus. *Curr. Microbiol.* 52:254–260. http://dx.doi.org/10.1007/s00284-005-0103-1

Singh, K., B. Bayrak, and K. Riesbeck. 2012. A role for TLRs in *Moraxella*-superantigen induced polyclonal B cell activation. *Front Biosci* (*Schol Ed*). 4:1031–1043. http://dx.doi.org/10.2741/S316

Snippert, H.J., A.G. Schepers, G. Delconte, P.D. Siersema, and H. Clevers. 2011. Slide preparation for single-cell-resolution imaging of fluorescent proteins in their three-dimensional near-native environment. *Nat. Protoc.* 6:1221–1228. http://dx.doi.org/10.1038/nprot.2011.365

So, N.S.Y., M.A. Ostrowski, and S.D. Gray-Owen. 2012. Vigorous response of human innate functioning IgM memory B cells upon infection by *Neisseria gonorrhoeae*. *J. Immunol.* 188:4008–4022. http://dx.doi.org/10.4049/jimmunol.1100718

Souwer, Y., A. Griekspoor, T. Jorritsma, J. de Wit, H. Janssen, J. Neefjes, and S.M. van Ham. 2009. B cell receptor-mediated internalization of salmonella: a novel pathway for autonomous B cell activation and antibody production. *J. Immunol.* 182:7473–7481. http://dx.doi.org/10.4049/jimmunol.0802831

Sperandio, B., B. Regnault, J. Guo, Z. Zhang, S.L. Stanley Jr., P.J. Sansonetti, and T. Pédron. 2008. Virulent *Shigella flexneri* subverts the host innate immune response through manipulation of antimicrobial peptide gene expression. *J. Exp. Med.* 205:1121–1132. http://dx.doi.org/10.1084/jem.20071698

Vaughan, A.T., A. Roghanian, and M.S. Cragg. 2011. B cells—masters of the immunoverse. *Int. J. Biochem. Cell Biol.* 43:280–285. http://dx.doi.org/10.1016/j.biocel.2010.12.005

Weller, S., M. Bonnet, H. Delagreverie, L. Israel, M. Chrabieh, L. Maródi, C. Rodriguez-Gallego, B.Z. Garty, C. Roifman, A.C. Issekutz, et al. 2012. $IgM^+IgD^+CD27^+$ B cells are markedly reduced in IRAK-4–, MyD88-, and TIRAP- but not UNC-93B-deficient patients. *Blood.* 120:4992–5001. http://dx.doi.org/10.1182/blood-2012-07-440776

Zivna, L., Z. Krocova, A. Härtlova, K. Kubelkova, J. Zakova, E. Rudolf, R. Hrstka, A. Macela, and J. Stulik. 2010. Activation of B cell apoptotic pathways in the course of *Francisella tularensis* infection. *Microb. Pathog.* 49:226–236. http://dx.doi.org/10.1016/j.micpath.2010.06.003